031169-1-T

Analysis of a Log-Periodic Folded Slot Antenna Array on Planar and Cylindrical Platforms

M.W. Nurnberger, S. Bindiganavale, L.C. Kempel,
J.L. Volakis and J. Mosko

Naval Air Warfare Center
Weapons Division
China Lake, CA 93555-6001

March, 1994

THE UNIVERSITY OF MICHIGAN
Radiation Laboratory
Department of Electrical Engineering
and Computer Science
Ann Arbor, Michigan 48109-2122
USA

Analysis of a Log-Periodic Folded Slot Antenna Array on Planar and Cylindrical Platforms

M. W. Nurnberger, S. Bindiganavale
L. C. Kempel, J. L. Volakis and J. Mosko *

Radiation Laboratory
Department of Electrical Engineering
and Computer Science
The University of Michigan
Ann Arbor, Michigan 48109-2122.

April 5, 1994

Abstract

This report describes the analysis of a Log-periodic Folded Slot Antenna (LPFSA). Using various computer codes, studies are performed on the effects of the various geometrical parameters on the antenna performance and resonance characteristics. On the basis of this study, a new design procedure is recommended for LPFSAs on planar platforms. In addition, cross-polarization radiation was evaluated and design curves were developed which show the effects of dielectric coatings and platform curvature when the LPFSA is deployed on cylindrical surfaces. Based on this preliminary study, predictable LPFSA designs can be developed.

*With the Naval Air Warfare Center, China Lake, CA 93555-6001

Contents

List of Figures

1 Introduction

Conformal antenna arrays are very attractive for aircraft, spacecraft, and land vehicle applications due to their inherent low weight and aerodynamic drag, and low cost, especially in comparison to conventional protruding antennas. The majority of the previous analytical studies focus on the development of planar conformal arrays, and those studies dealing with actual non-planar conformal antennas have been based predominately on experiment due to a lack of rigorous analysis techniques. Also, most of the research has been directed towards the study of patch arrays which are inherently narrow band.

Due to the large bandwidth, high gain, and pattern coverage requirements, a logarithmically periodic antenna is a natural choice. The design methodology for the most common antenna of this type, the Log-Periodic Dipole Array (LPDA), has been developed by Carrel [1], and is very well known. Unfortunately, it is not applicable to the problem at hand, as it involves the use of protruding elements, which are non-conformal. Greiser [2] has presented an antenna based on the same principles, but using a folded-slot element for conformal mounting. As will be shown, the assumptions made by Greiser in the design of his antennas, while perfectly valid for an antenna utilizing straight wire dipoles such as the LPDA, are not directly applicable to the folded slot elements. Hence, a new design procedure must be developed for these antennas. The antennas based on this new design procedure will be henceforth denoted Logarithmic Periodic Folded Slot Arrays or LPFSAs.

The goal of this project is to further the state-of-the-art in the design and analysis of singly- and doubly-curved conformal slot antennas, and to design and develop an optimum ultra-wide-band conformal array of LPFSA's for placement around the nose of a missile (see Figure 1), while accommodating a terminal device located in the center of the nose. It is envisioned that at least four LPFSAs must be placed around the nose for sufficient coverage, but up to eight LPFSAs may to needed to satisfy other requirements.

The biggest challenge in the analysis and design of the proposed LPFSAs is a lack of suitable software for slot antennas. Although a variey of software are available for wire antenna analysis, there is a dearth of slot antenna software. Moreover, even greater challenges exist in assessing the effects of curvature, substrate, and cavity absorber on the performance of the LPFSA.

Nevertheless, during the period of the project (spanning eight months), a sufficient body of data was collected which can be readily consolidated and used to develop a good design on a curved platform. The data was collected by using the wire code NEC [3], a planar finite element analysis code [4] [5], and a new preliminary finite-element code [6] which permits modeling of slot antennas on cylindrical platforms. This code, although inefficient for this application, proved invaluable in establishing design curves which account for curvature and substrate effects.

2 Geometry Description

The planar LPFSA is a logarithmically periodic array of co-planar folded slot elements, series-fed from the high-frequency end, as shown in Figure 2. Figure 2 shows the originally supplied LPFSA, designed using the standard LPDA procedure developed by Carrel. This geometry was adapted for modelling with the finite element codes at the University of Michigan, as shown in Figure 3. As will be discussed later, because of the narrow slots our present finite elements are inefficient for this analysis and thus an equivalent wire model was also developed (the LPFDA), for a more efficient analysis of the antenna via the method of moments. This geometry is shown in Figure 4.

3 List of Studies

To more completely understand the operation of the LPFSA, several smaller individual investigations were carried out.

Initially, a single folded slot was studied in depth, to more fully understand its operation (input impedance, bandwidth, pattern, etc.). This involved studies on the effect of the slot width and separation, as well as the effects of a thin dielectric substrate on the impedance characteristics of the folded slot. The current density on the equivalent folded wire dipole was also studied extensively, since its phase variation is crucial to the proper design of the array. The dependence of the radiation pattern on the slot separation was also examined.

Concurrently, the effects of curvature on both the impedance and radiation characteristics of the folded slot were evaluated using a newly-developed

FEM code [6].

Finally, based on the results of the individual parameter studies, a new design procedure was developed that produces a more optimal antenna with respect to gain, radiation pattern coverage, and input impedance.

4 Planar Antenna Parameter Studies

To gain a better understanding of the underlying operation of the LPFSA, as mentioned above, the planar folded slot element was first studied in great detail, as it is the fundamental building block of the LPFSA. The input impedance of the folded slot was determined as a function of the slot width and separation and the effect of the substrate on the resonance of the folded slot was quantified. Also, a new code was used to determine the effect of platform curvature on the resonance frequency. The individual element currents were studied in some detail to determine the phasing effects of each element on the antenna feeding structure, and the dependence of the radiation pattern on such parameters as slot separation was determined. In reality, as will be explained shortly, the Babinet's principle equivalent folded dipole was actually modelled.

4.1 Slot-Wire Equivalence

As mentioned above, due to numerical inefficiency, it was necessary to substitute an equivalent wire geometry for the actual geometry, i.e. to replace the slots with their equivalent dipoles. Theoretically, Babinet's principle allows for the substitution of a complementary strip dipole for a slot in an infinite-extent perfectly conducting ground plane. Then, for a slot/strip width $w \ll \lambda$, the strip can be approximated with a dipole of radius $a = w/4$. Figure 5 gives a diagrammatic description of this approximation.

To prove the validity of this substitution several comparisons were made. Before the actual folded elements were compared, the simplest case of a single slot and its equivalent dipole were considered. Numerical results from either case were compared with analytical results and found to be in very good agreement. This comparison not only served to verify the assumptions made in the slot-dipole equivalence, but also to establish the accuracy of the employed numerical simulation codes.

Following the initial verification, the input impedance of the two equivalent folded elements over a range of frequencies were compared. As can be seen in Figure 6, both the real and the imaginary parts of the input impedance compare very well, again proving the validity of the assumptions made in the substitution.

The input impedance of the full seven-element array was also calculated with both simulation codes. As Figure 7 demonstrates, the values calculated by the two codes agree very well. Henceforth, unless otherwise specified, the terms "slot" and "dipole" will be used interchangeably.

4.2 Slot Width

The effects of the slot width, or equivalently, the wire radius, on the input impedance were numerically evaluated. Theoretical predictions indicate that as the radius of a dipole increases, its bandwidth also increases i.e. the dipole becomes less resonant. This is verified using Figure 8 which shows that the real part of the input impedance at resonance decreases for thicker dipoles.

4.3 Slot Separation and Bandwidth

Figure 8 also demonstrates a characteristic of the folded dipole that is generally not exploited. In general, a dipole is folded only to modify its input impedance for impedance- matching purposes, and any resulting increase in the bandwidth is a happy circumstance. A folded dipole of this type typically has a separation on the order of $\lambda/150$, and a bandwidth of less than 15%. The folded dipole under study, however, has a separation of approximately $\lambda/10$, and an approximate impedance bandwidth of 35%, making it extremely wideband.

This increase in bandwidth is a result of the large separation between the two parallel radiating wires. For the typical folded dipole, the two radiating wires are placed very close together. This allows the unbalanced (radiating) component of the current to be modeled by a singe wire of larger radius. However, for the element under study, the two radiating wires are too far apart and cannot be considered as a single element. The current on each of the radiating wires is composed of two components - the current impressed by the source, and the current induced through coupling. Ignoring for the moment the transmission-line mode currents, which do not radiate,

the unbalanced (radiation) currents impressed by the source will have the same phase in either wire - the first resonance occurs when the element is approximately one wavelength in circumference, forcing the currents to be symmetric. However the currents induced by the field from the other radiating wire will not be in phase with the induced currents, as they incur a phase lag due to the distance they must travel. The end result is that at any time the unbalanced (or radiating) currents on the antenna do not add entirely constructively. There is some destructive interference resulting from the phase lag of the induced currents. Hence, any sharp resonance peaks will be somewhat canceled, and an overall smoothing of the impedance behavior around resonance will be observed.

As a result of another study, a narrower folded slot was also considered. As can be observed from Figure 9, the bandwidth has decreased, verifying the conclusions drawn above. Figure 9 also demonstrates another result of modifying the slot separation. We observe that as the slot separation decreases, the resonant frequency increases. In this case, the separation is decreased by 50% and the resulting increase in resonant frequency is approximately 11%. This resonance shift is not terribly critical, but must be quantified to ensure adequate coverage at the ends of the specified operational frequency range.

4.4 Substrate Effects

The substrate effect on the resonance frequency of the folded slot was evaluated by using the finite element program CAVITY3D [4]. This code analyzes the radiation of cavity-backed antennas. To accomodate the code requirements the slot was modeled as in Fig 25. Having numerically verified the slot-dipole equivalence and its associated assumptions, the effects on the resonance frequency and input impedance of the substrate on which the folded slot is fabricated were examined. As was expected, the substrate lowers the resonance frequency. As shown in Figure 10, for the dielectric of thickness $t = 0.010"$ and $\epsilon_r = 4.8$, the shift in resonance is approximately 300 MHz. Clearly, as the dielectric constant of the substrate is increased, the resonant frequency will continue to decrease. Similarly, increasing the substrate thickness or decreasing the slot width will have the same effect. Qualitatively, the resonant frequency decreases as the root of the dielectric constant, the substrate thickness, or the slot width are increased.

4.5 Folded Element Currents

To more fully understand the operation of the LPFSA, it is necessary to explain the current distribution on each element, and how each element interacts with the transmission line that feeds it. A diagram of the feeding scheme for the LPDA is shown in Figure 11. As can be seen, the array is fed from the high-frequency end, and the energy propagates along the loaded parallel-wire line until it encounters one or more dipoles that are approximately resonant length. To synthesize a smooth, well-behaved pattern, it is necessary to direct the radiated energy away from the larger elements which might otherwise be excited through mutual coupling. The appropriate inter-element phasing to achieve this relies on the selection of the distance between the adjacent elements and the polarity reversal at the feed of each element.

The LPFSA also depends on this backfire mode of operation to attain smooth, well-behaved patterns. However, as shown in Figure 12, because the individual elements are fed in series, the feed polarity reversal cannot be achieved by simply reversing the feed connections. Instead, advantage is taken of the physical geometry of the element, and the polarity reversal accomplished by forcing the energy to travel around the element, which is approximately one-half a wavelength.

To determine the actual phase shift imparted by this detour, an in-depth study of the currents on the folded dipole element was performed. As shown on the x-y plane of the 3-D plot in Figure 13, a folded dipole was placed in the middle of a long parallel-wire line terminated to minimize reflections. The currents on the wires were then calculated and plotted.

As Figure 13 shows, neither the input or output transmission lines were matched to the element, nor did the termination work properly. Because the input and output transmission lines were chosen to be equivalent to those used in the LPFSA, they were not modified. However, the reflections on the output line were large enough to affect the current phase measurements. Hence, a brief study of termination methods in NEC was conducted. The termination that yielded the lowest standing-wave ratio (SWR) was a resistor distributed over the full width of the parallel-wire line. The results of this termination are shown in Figure 14. Comparison of Figures 13 and 14 shows a decrease in the SWR from 1.49 to 1.03.

Having obtained a valid current distribution on the folded dipole element, the phase of the currents at the input and output of the folded dipole were

examined and found to be somewhat less than 180^0 out of phase. This is to be expected, as the distance the current must travel is somewhat less than the circumference of the antenna. This result verifies to some extent the proposed phasing solution mentioned above, but also suggests a more accurate approach. Besides the phase shift imparted by the detour around the folded element, additional phase difference must be introduced to ensure a 180^0 phase shift between adjacent elements. This requirement drives the antenna design procedure which is presented later.

4.6 Coupling Study

According to a last-minute request, the coupling between two LPFDA arrays (in proximity) was also investigated. The design parameters of the originally supplied LPFSA were used to determine the orientation of the two antennas. In this case, they were placed tip-to-tip with their axes forming an angle of 45^0, as shown in Figure 15. However, due to numerical constraints, two full LPFDA arrays were not used. Instead, one full LPFDA array was used, and a folded dipole element at the appropriate orientation and position was used in place of the other. The coupling calculations were deliberately made at 2.75 GHz, where both antennas are most resonant, to give a worst-case figure of approximately -22 dB.

The validity of the substitution of the single folded dipole for the full LPFDA was verified by also computing the mutual coupling between two identical folded dipole elements in the same relative positions. Again, the worst case figure obtained was approximately -21 dB. It is not surprising that the coupling between the two folded dipoles is higher than that between the LPFDA and the folded dipole. The LPFDA is a higher gain antenna, and is thus associated with sharper and narrower radiation patterns, i.e. less energy is directed to the sides, where it may couple with other antennas. By similar reasoning, the coupling between two LPFDA's should be even lower, because both antennas are quite directive, and even less energy would be available on the sides, where it can couple with other antennas.

4.7 Gain Study

A brief study was also made of the overall antenna gain dependence on antenna length. The results given in Figure 16 are approximate values for the

LPDA. However, they are indicative of a minimum performance criterion for the LPFSA designed with the new procedure discussed above. As discussed elsewhere in this report, increasing the length of the antenna offers many advantages, among them increased gain, lower mutual coupling, better packing density around the airframe, more optimum impedance performance, and others.

5 Modified Design Procedure

As was mentioned several times above, the implementation of the LPFSA is somewhat different than that of the LPDA for a number of reasons. While the elements of the LPDA (half-wave dipoles) have effectively zero width, the elements of the LPFSA (half-wave folded slots) are of finite width. Also, because the LPDA is a parallel array of half-wave dipoles, it is easy to achieve the progressive polarity reversal at each element by reversing the feed connections. The LPFSA, on the other hand, is a series-fed array, and must derive the progressive polarity reversal mentioned above in some other fashion. Either of these factors are enough to invalidate the original design procedure developed by Carrel [1], and are the driving force behind the development of a new design procedure for the LPFSA.

5.1 Ideal LPDA performance

Figure 17 shows the LPDA nomenclature, and gives the design parameter relations governing the critical dimensions of the antenna. The complete design procedure is given by Carrel [1]. Figures 18 and 19 give the computed performance of an LPDA designed with the same parameters ($\tau = 0.8, \alpha = 40^0, \sigma = 0.137$) as the antenna originally supplied, except that the operational bandwidth was truncated, as discussed previously. Figure 18 demonstrates the log-periodic antenna characteristic impedance variation with the logarithm of frequency, in the operating frequency range of the antenna - in this case, between 2.0 and 3.0 GHz. Figure 19 gives some indication of the actual performance of the antenna, showing the power delivered to the antenna. Equivalently, if the antenna is lossless and has an efficiency of 100%, which are justifiable approximations in this case, then Figure 19 shows the relative gain of the antenna vs. frequency. It is interesting to note

that although the impedance variations in Figure 18 appear quite large, they have a small effect on the actual performance of the antenna (see Figure 19). It should also be pointed out that these impedance variations may be smoothed out somewhat by modifying the design parameters to give a longer antenna with more elements.

5.2 Performance of the Original LPFDA Design

The originally supplied LPFDA was modeled using the NEC code to examine its performance, and the results are shown in Figures 20 and 21. In Figure 20, the input impedance seems to vary unpredictably, sometimes rising to very high values, and the power transmitted as a function of frequency (Figure 21) ia also quite erratic. In comparison with the plots given in Figures 18 and 19 for the ideal LPDA, these plots indicate a serious oversight in the design of the original LPFSA.

As mentioned above, the finite width and length of the folded slot elements must be accounted for in the design procedure to achieve the necessary phase shift between elements. Further study and measurements of the originally supplied LPFSA indicated that this factor had not been adequately taken into account.

5.3 Modified LPFDA design technique

Based on our knowledge to this point, the spacings between the elements of the LPFDA were modified to included the folded dipole width. The specifics of this are given in Figure 22, as well as a pictorial indication of the effects of the modifications to the antenna geometry. The electrical effects of these modifications are shown in Figures 23 and 24.

5.4 Modified LPFDA Performance

The performance of the new LPFDA design (see Figures 23 and 24) is significantly better in several aspects. The input impedance is much more predictable, both in amplitude and period, and the power transmitted is considerably more consistent and predictable across the operating frequency of the antenna. However, in comparison with their ideal LPDA counterparts,

Figure 23 still shows some instability in the input impedance, and Figure 24 indicates that the transmitted power has deeper nulls.

It is also instructive to compare the relative input impedance levels between the ideal LPDA and the modified LPFDA. The LPDA's input impedance seems to vary consistently between approximately 200 and 450Ω, while the LPFDA's input impedance varies over a considerably larger range; between approximately 150 and 800Ω. The difference in ranges and values should be attributed to the different elements of the array. While the half-wave dipole (in the LPDA) has an input impedance of approximately 72Ω at resonance, the folded half-wave dipole has an input impedance which is 4 times larger.

6 Cylindrical Platform Analysis

6.1 Code Description and Model Definition

The single folded slot on a cylindrical platform was analysed using fema_cyl, a finite element-boundary integral code for analysis of radiation and scattering by cavity-backed structures in an infinite metallic cylinder, developed at the University of Michigan [6]. The geometry of the slot with the dielectric substrate and in the presence of the absorber-loaded cavity is shown in Figures 25 and 26, when the slot is mounted on a planar platform. When mounted on a cylindrical platform the geometry is as depicted in Figure 27. The modeling of the aperture as a collection of metallic patches is shown in Figure 28 and the aperture after discretization is shown in Figure 29. While finding the slot impedance as a function of frequency, the transcript of a typical session with fema_cyl is given in Appendix A.

6.2 Curvature Effects

The variation of the slot impedance as a function of frequency for different platform diameters is shown in Figure 30. It is observed that the curvature of the platform does not affect the resonance frequency appreciably. There is only a 100 MHz shift in the resonance frequency between the two extreme curvatures of interest (the planar and the 6" diameter cases). In order to reduce the cross-polarization a second slot, with a slot separation of 0.38608

cm, was also analysed. The resonance frequency for this slot on the planar platform was 1.82 GHz whereas mounting on a 6" diameter cylinder yielded a resonance frequency of 1.9 GHz as seen in Figure 31.

6.3 Radiation Patterns

The principal planes for the radiation patterns are as defined in Figure 32. The H-plane and E-plane patterns with the slot separation of 0.77216 cm for different platform diameters are shown in Figures 33 and 34. The E-plane patterns are very broad as would be expected. Similar patterns for the slot with the smaller slot separation are shown in Figures 35 and 36. The cross-polarization levels for this case are much lower than the previous case.

7 Summary and Conclusions

The purpose of this study was to investigate the radiation properties of Log-Periodic Folded Slot Antennas(LPFSAs) mounted on a doubly curved (missile-like) platform. A goal was also to develop a preliminary design of the LPFSA.

Since there are no available design procedures for LPFSA antennas, other than a recommended sketch based on the patent by Carrel[1], our first effort concentrated on the understanding of the antenna's operation. For this purpose an equivalent wire model of the LPFSA was developed and simulated using the NEC code. Both a single folded slot and a 7-element LPFSA was studied extensively. This study revealed the role of the different geometrical parameters and led to a new design procedure which renders predictable performance. This was verified analytically but as yet no measurements have been collected using configurations based on the new design. It was also verified that the slot width plays a role in the radiation characteristics of the folded element. In particular we found that a slot width of 0.012 λ was more desirable.

Perhaps the more difficult part of this investigation dealt with the evaluation of the curvature and substrate effects. This was because of a lack of available software for non-planar antennas. However, a recently completed finite element code at the University of Michigan proved very useful for this application. This code was adapted to analyze the folded slot dipole in the

presence of the absorber-loaded cavity and dielectric substrate. Although the finite element code was inefficiently used because the slot was extremely small in comparison to the cavity, given the short time limitations, this was our only alternative. Using U-M's finite element code, the curvature and dielectric constant effects on the resonant length of the folded slot were quantified within the parameter range of interest. Also, the same code was used to study and quantify the cross polarization radiation. It was found that smaller slot widths and spacings between the folded slot arms were necessary to lower the cross polarization returns which could be kept to less that -25dB without great compromises. It was also found that the front to back ratio was 25dB or better.

In conclusion, based on this initial study we have demonstrated that the LPFSAs can be predictably designed to meet given specifications on gain, bandwidth, cross-polarization and pattern coverage. In addition, it was determined that pairs of closely printed LPFSAs have a low coupling of less than -20dB.

8 Future Work

The data provided in this report along with a few more curves generated from our present codes can indeed be used to develop a good and "safe" array design. However, it is instructive that additional analysis and studies be performed before proceeding with antenna prototypes. Specifically, the following tasks are recommended:

1. Refinement and validation of the new design procedure for LPFSA. This task will require additional numerical testing in addition to an experimental validation. So far 7-element design has been used in our analysis. However, this needs to be extended to a 15+ element LPFSA to cover the required 2-18 GHz band. Also, a new experimental set up must be employed to eliminate extraneous ground plane diffractions which have so far contaminated the measured patterns.

2. Develop an efficient code for generic slot arrays on cylindrical platforms. This new finite element code is necessary for the efficient analysis of slot antennas on cylindrical platforms. The completion of this code will be the first step towards the development of a code for slot antenna

designs on a doubly curved platform. The development of this code is not difficult but will be quite important in developing a very reliable antenna design suitable for full scale deployment. Using this code, the substrate effects, cavity backing, platform curvature, slot width, and cross-polarization can be taken into account concurrently. A prototype will be also build as part of this task to validate the code and selected design. This code will be suitable for the analysis of several elements on the cylindrical platform and can also be used to account for the changing curvature of the conical platform by making several runs of the code. Moreover this code can take into account the presence of dielectrics which can be used to reduce the element size and consequency allowing for performace improvements not otherwise possible with the present platform and cavity size constraints. Other, related studies, have also shown that the individual or pairs of LPFSAs must be placed on separate cavities for RCS reduction as demonstrated in Figure 37.

3. Develop an efficient design code for slot antennas on conical platforms. This is the "ultimate" design code for slot arrays on doubly curved platforms and will be an important contribution in the field of slot array design. However, the completion of its implementation cannot be promised before the end of calender year 1994. The completion of this code can be promised by March-April 1995 and it may therefore be useful for design improvements and validations before final deployment.

4. Construction of an experimental prototype and code verification. This task must be an integral part of the code development discussed under Tasks 2 and 3. Given the lack of available data for LPFSAs, the code development cannot be completed without extensive validation at various stages. Consequently, it will be necessary to build and test LPFSA prototypes at leat on cylindrical platforms for code validation before delivery. By using a cylindrical platform, the fabrication cost is substantially reduced(can be done with a few hundred dollars). The actual testing can be done either at the University of Michigan or at the sponsor's facilities.

References

[1] Carrel, Robert L., "Analysis and Design of the Log-Periodic Dipole Antenna," Ph.D. Dissertation, *University of Illinois*, Urbana, IL, 1961.

[2] Greiser, John W., "Log-Periodic Antenna Structure," *U.S. Patent* 3,369,243, Feb 3, 1968.

[3] Burke, G.W., Poggio, A.J., "Numerical Electromagnetics Code (NEC) - Method of Moments," *Lawrence Livermore National Laboratory*, Rept. UCID-18834, January 1981.

[4] Jin, J.M., Volakis, J.L., "A Hybrid Finite Element Method for Scattering and Radiation by Microstrip Patch Antennas and Arrays Residing in a Cavity," *IEEE Trans. Antennas and Propagat.*, Vol AP-39, No. 11, Nov 1991.

[5] Jin, J.M., Volakis, J.L., "Electromagnetic Scattering by and Trasmission Through a Three-Dimensional Slot in a Thick Conducting Plane," *IEEE Trans. Antennas Propagat.*, Vol AP-39, No. 4, Apr 1991

[6] Kempel, Leo C., Volakis, John L., Bindiganavale, Sunil S., "Radiation and Scattering from Printed Antennas on Cylindrical Conformal Platforms," *University of Michigan Radiation Lab*, Report 030601-3-T, Jan. 1994.

9 Appendix A

The transcript of a typical session with fema_cyl while finding the slot impedance as a function of frequency, is given below :

```
||||||||||||||||||||||||||||||||||||||||||||||||||||||||||
|                                                        |
|                    FEMA_CYL                            |
|                                                        |
| A program for antenna arrays on metallic cylinders     |
|                                                        |
|               Radiation Laboratory                     |
|              University of Michigan                    |
|                                                        |
| Copyright:  The Regents of the                         |
|             University of Michigan     (1993)          |
|                                                        |
||||||||||||||||||||||||||||||||||||||||||||||||||||||||||


|||||||||||||||||||||||||||||||||||||||||||||||
|           Memory Demand                      |
|||||||||||||||||||||||||||||||||||||||||||||||

Integer arrays requires:   22.04013     MBytes
Real    arrays requires:  2.0800000E-04 MBytes
Complex arrays requires:   24.44435     MBytes

ESTIMATED TOTAL MEMORY DEMAND >   46.48469     Mbytes


Do you wish to run:
                    1) Preprocessor
                    2) FEM-BI
                    3) Impedance aperture
                    0) Exit
```

```
1

 Performing initialization, please wait....

 Enter radius of cylinder (cm):
8.125
 Enter array size (phi,z) in (deg,cm):
127.9600571 13.31976
 Enter center of array (phi,z) in (deg,cm):
0 0
 Enter number of grid points in (phi,z) direction
48 70

 Discretization:
                 deltaPhi =    2.722554     deg
                 deltaZ   =   0.1930400     cm

 Enter number of cavities in phi,z directions
1 1

 Enter number of nodes per cavity (phi,z):
48 70


        3360 surface nodes have been generated...
 The node numbering has the following pattern

 SINGLE CAVITY:

   ^
   |   21   22   23   24   25
   |   16   17   18   19   20
   z   11   12   13   14   15
   |    6    7    8    9   10
   |    1    2    3    4    5
   ---------- phi ---------->
```

```
 if for example 25 nodes were specified.
 where node 13 is the center point.


 Now specify which other nodes are either:
             metallic
                or
             resistive

 All surface nodes metal or resistive (1=yes):
0
Are the nodes substrate nodes (1=yes):
0
 Enter number of metallic patches:
5
 Enter row,column of lower left corner of
 the patch on uniform grid for patch:          1
0 0
 Enter number of unknowns(edges) for each
 dimension (phi,z):
47 32
 Enter row,column of lower left corner of
 the patch on uniform grid for patch:          2
32 0
 Enter number of unknowns(edges) for each
 dimension (phi,z):
16 5
 Enter row,column of lower left corner of
 the patch on uniform grid for patch:          3
32 31
 Enter number of unknowns(edges) for each
 dimension (phi,z):
16 5
 Enter row,column of lower left corner of
 the patch on uniform grid for patch:          4
37 0
 Enter number of unknowns(edges) for each
```

```
 dimension (phi,z):
47 32
 Enter row,column of lower left corner of
 the patch on uniform grid for patch:          5
33 17
 Enter number of unknowns(edges) for each
 dimension (phi,z):
13 3
 Enter number of substrate layers(INTEGER):
7

 Generating sub-surface nodes....
 Enter layer            1 thickness (cm):
.0254
 Enter layer            2 thickness (cm):
1.125
 Enter layer            3 thickness (cm):
1.125
 Enter layer            4 thickness (cm):
1.125
 Enter layer            5 thickness (cm):
1.125
 Enter layer            6 thickness (cm):
1.125
 Enter layer            7 thickness (cm):
1.125

 Do you want to save this geometry (1=yes):
1
 Enter FEMA_CYL filename:
a8125.cyl
 Do you wish to run:
                    1) Preprocessor
                    2) FEM-BI
                    3) Impedance aperture
                    0) Exit
 2
```

```
 Performing initialization, please wait....

 Enter EXCALIBUR filename:
a_8125.cyl
 Reading excalibur file: a_8125.cyl

 Material Parameter Specification....
 Is the material filling constant (1=yes,0=no)?
0
 Each layer of elements constant (1=yes,0=no)?
0
 Well, each element must be individually entered...
 Entry by keyboard or file (1=key,0=file)?
0
 Material file must have structure:
 Re[epsilon] Im[epsilon] Re[mu] Im[mu]
 There must be at least         22701lines.
 (one line per element)

 Enter material filename:
mat_spec_file

 Checking dimension allocations...

 Number of Boundary Integral Unknowns:          36
 Total number of UNKNOWNS:       60152

Enter tolerance, minimum and maximum iterations:
.01 2 10000
Do you wish to monitor convergence (0=no,1-yes)?
1
 Do you want:  0 = no preconditioning, 1 = diagonal?
1
 Do you want to compute:
      0 = RCS/Pattern, 1 = Zin, 2 = Freq. Sweep?
2
```

```
 Enter Zin filename:
slotzin
 Enter Frequency sweep data filename:
freqsweep
 Enter observation type:
                          0) Backscatter
                          1) Bistatic
                          2) Radiation
2
 Enter start,stop, and increment azmuth angles [deg]:
0 0 1

 Enter start,stop,and increment elevation angles [deg]:
90 90 1

 Enter ouput RCS filename [<= 40 characters]:
junk
 ||||||||||||||||||||||||||||||||||||||||
 |     PROBE FEED INFORMATION            |
 ||||||||||||||||||||||||||||||||||||||||

 Enter number of feeds:
1
 Enter feed direction (1=rho, 2=phi, 3=z):
3
 Enter feed location (rho,phi) in (cm,deg):
8.124999 0
 Enter center point of feed (cm):
-.57912
 Enter layer number of feed <=:          7
1
 Enter mag,phase of probe current (amp,deg):
1 0
 ||||||||||||||||||||||||||||||||||||||||
 |     IMPEDANCE LOAD INFORMATION        |
 ||||||||||||||||||||||||||||||||||||||||
```

```
 Enter number of loads:
0
 Enter start,stop and increment freq. (GHz):
1.4 2.4 .1
Do you wish to run:
                      1) Preprocessor
                      2) FEM-BI
                      3) Impedance aperture
                      0) Exit
0
```

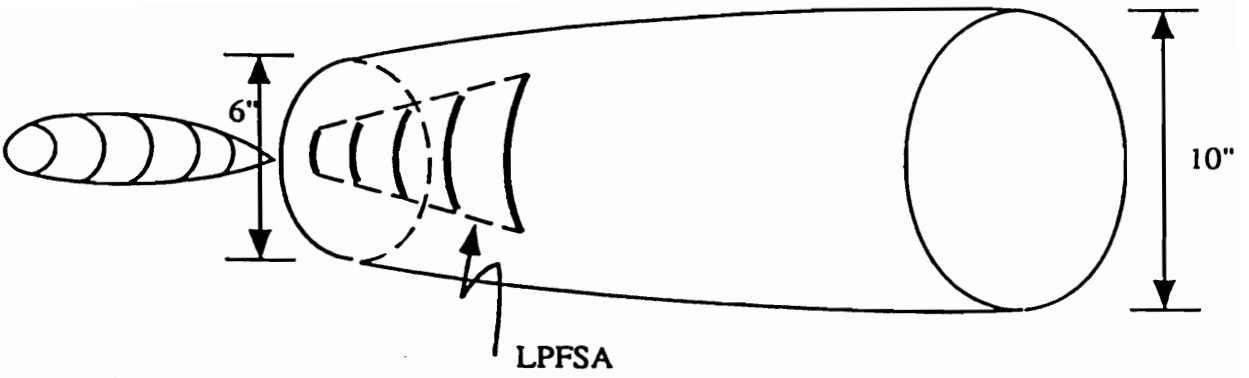

Figure 1: Example placement of conformal LPFSAs around the missile cone

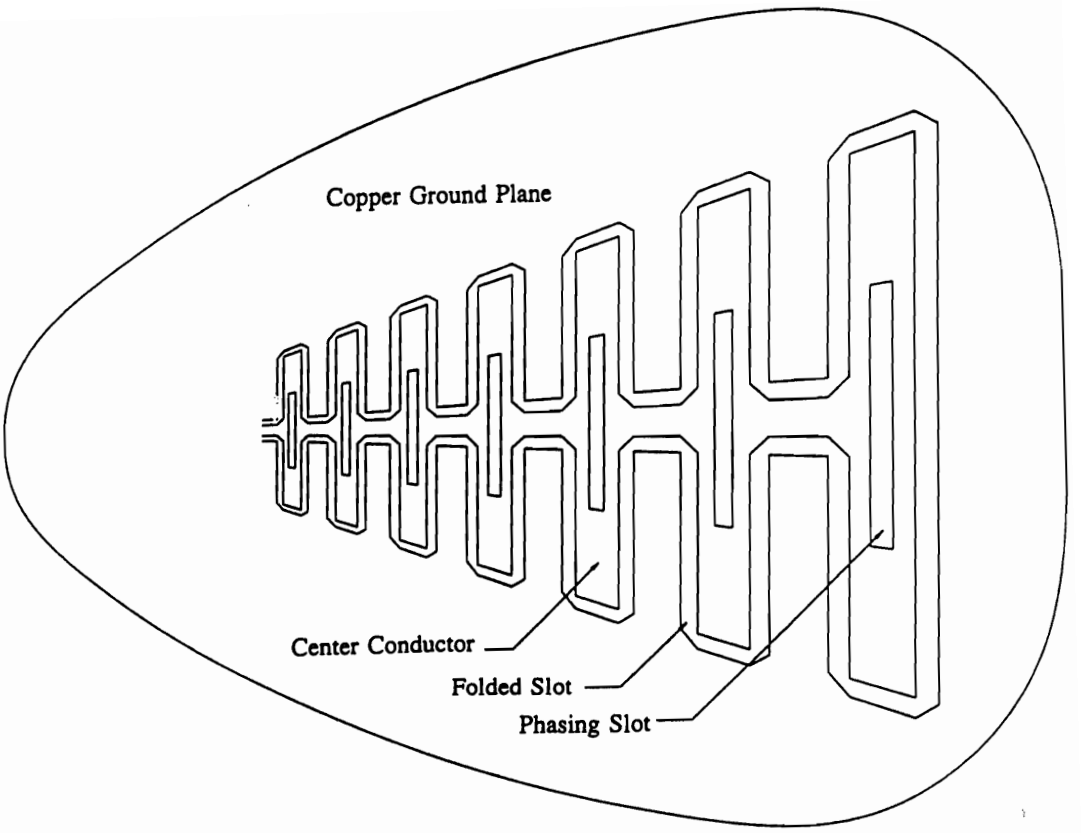

Figure 2: Truncated version of the originally supplied LPFSA

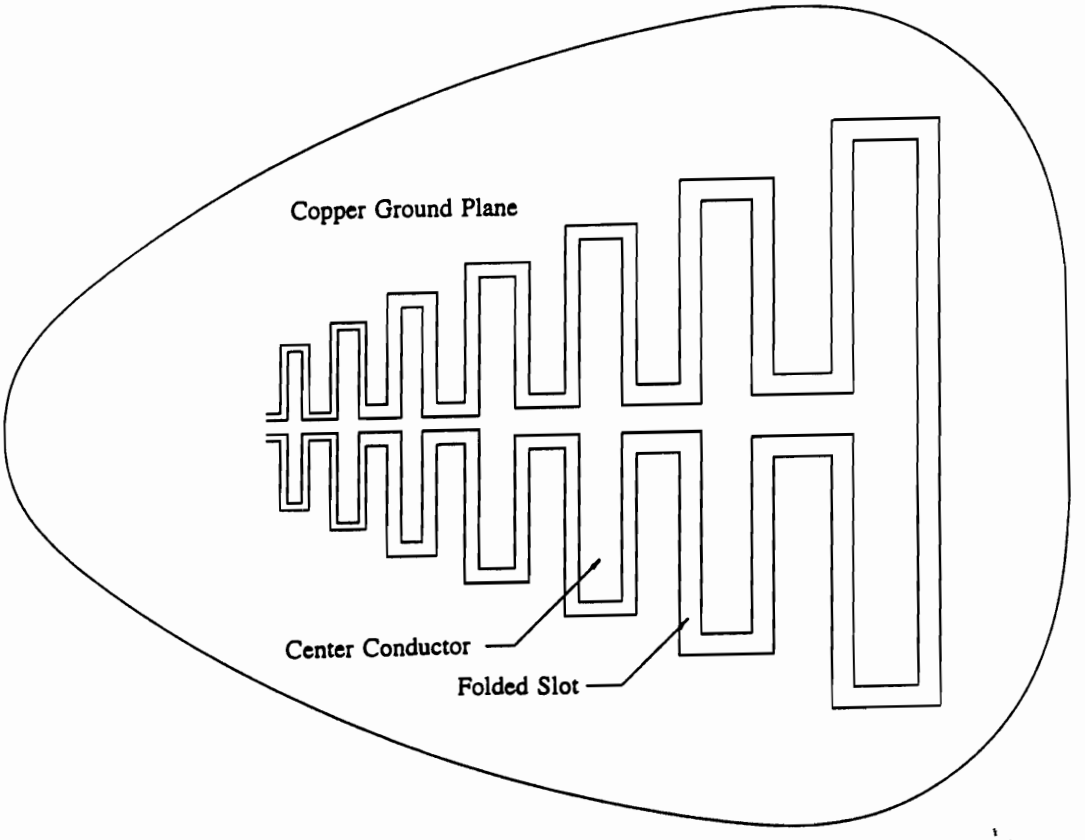

Figure 3: Adaptation of originally supplied LPFSA for ease of modeling

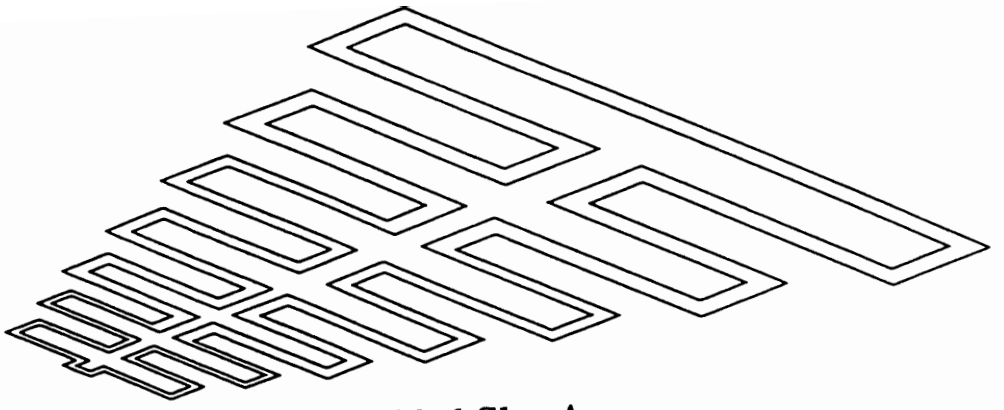

Folded Slot Array

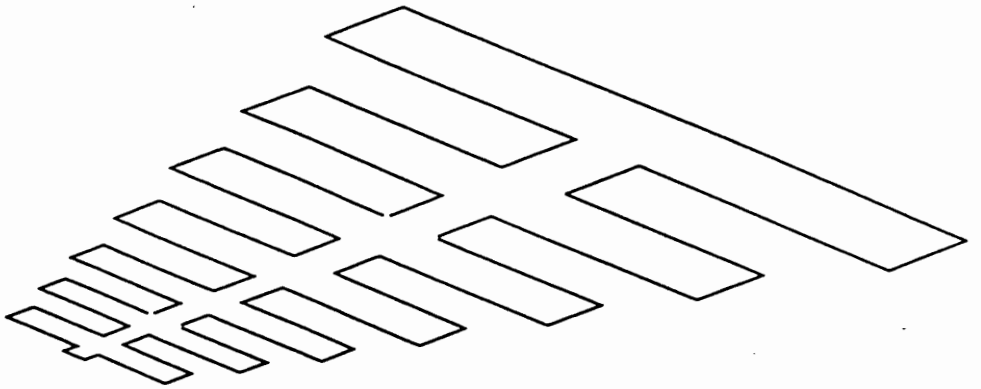

Folded Dipole Array

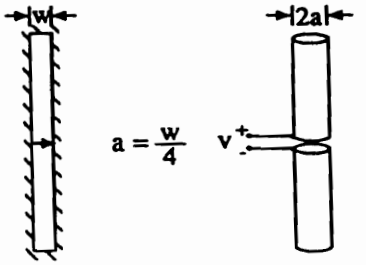

Equivalence Relation

Figure 4: Equivalence of LPFSA and LPFDA

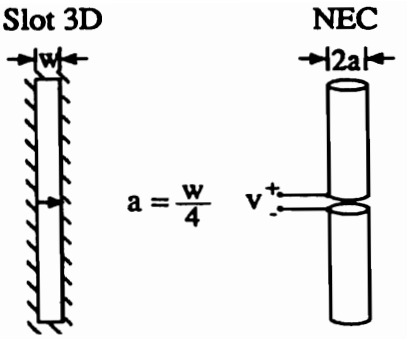

Figure 5: Dipole/slot equivalence relation

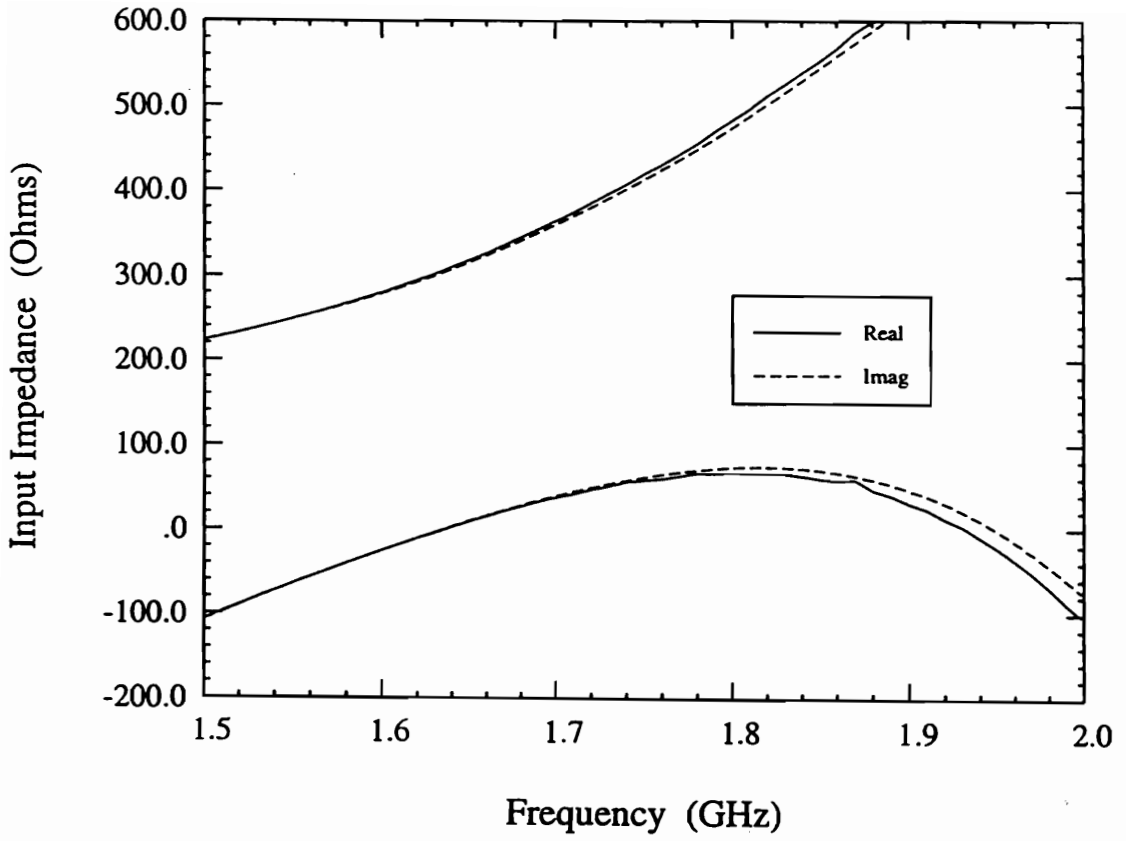

Figure 6: Dipole/slot input impedance validation

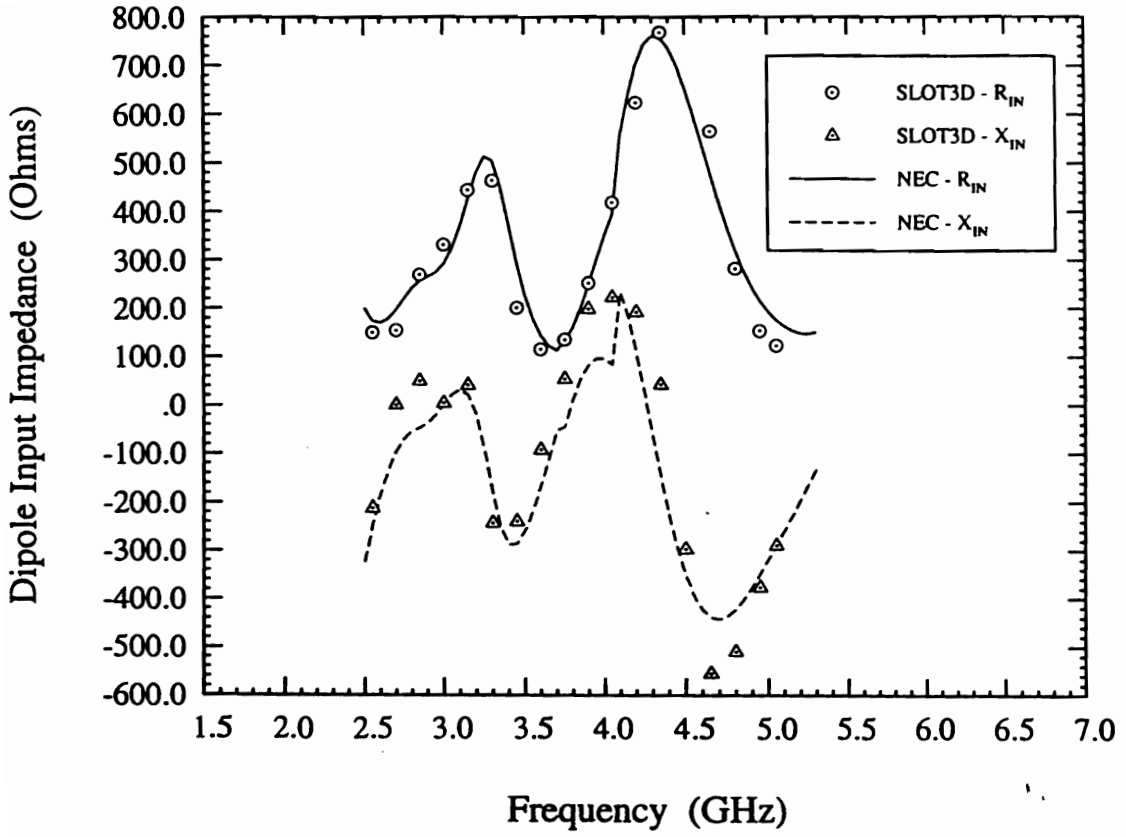

Figure 7: Slot3D - NEC impedance validation

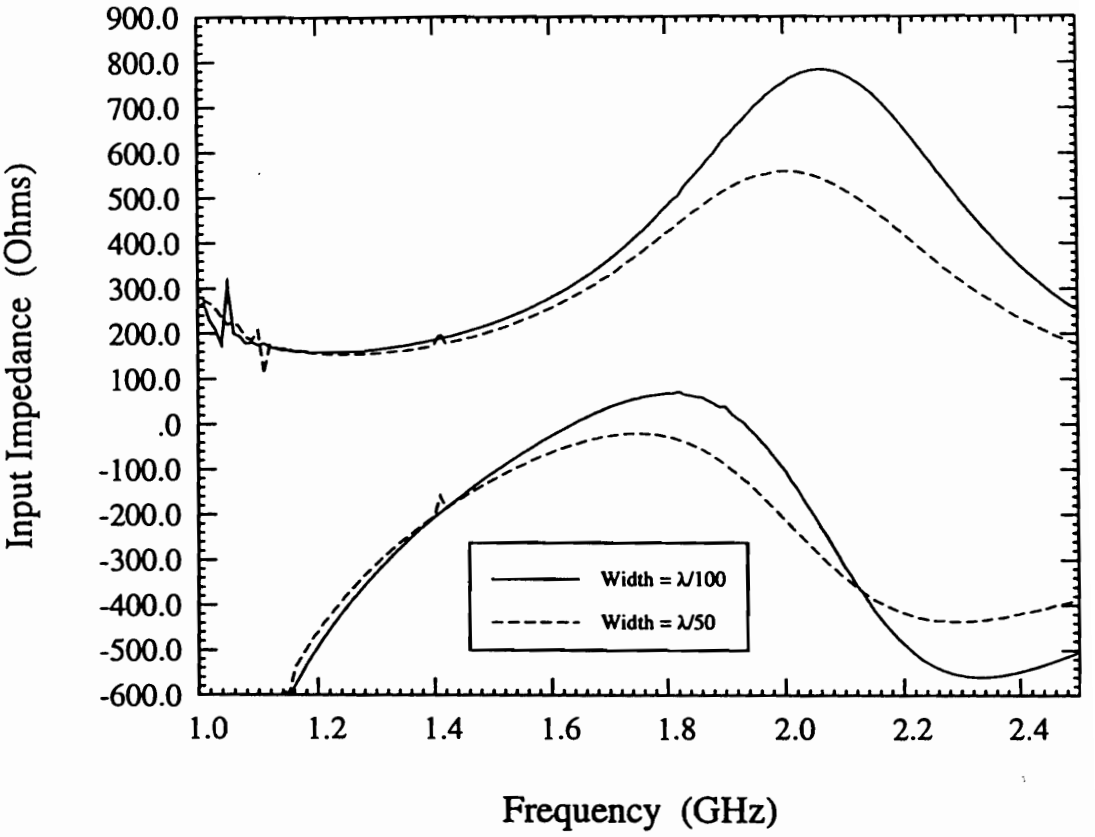

Figure 8: Variation of the input impedance of the folded slot with slot width

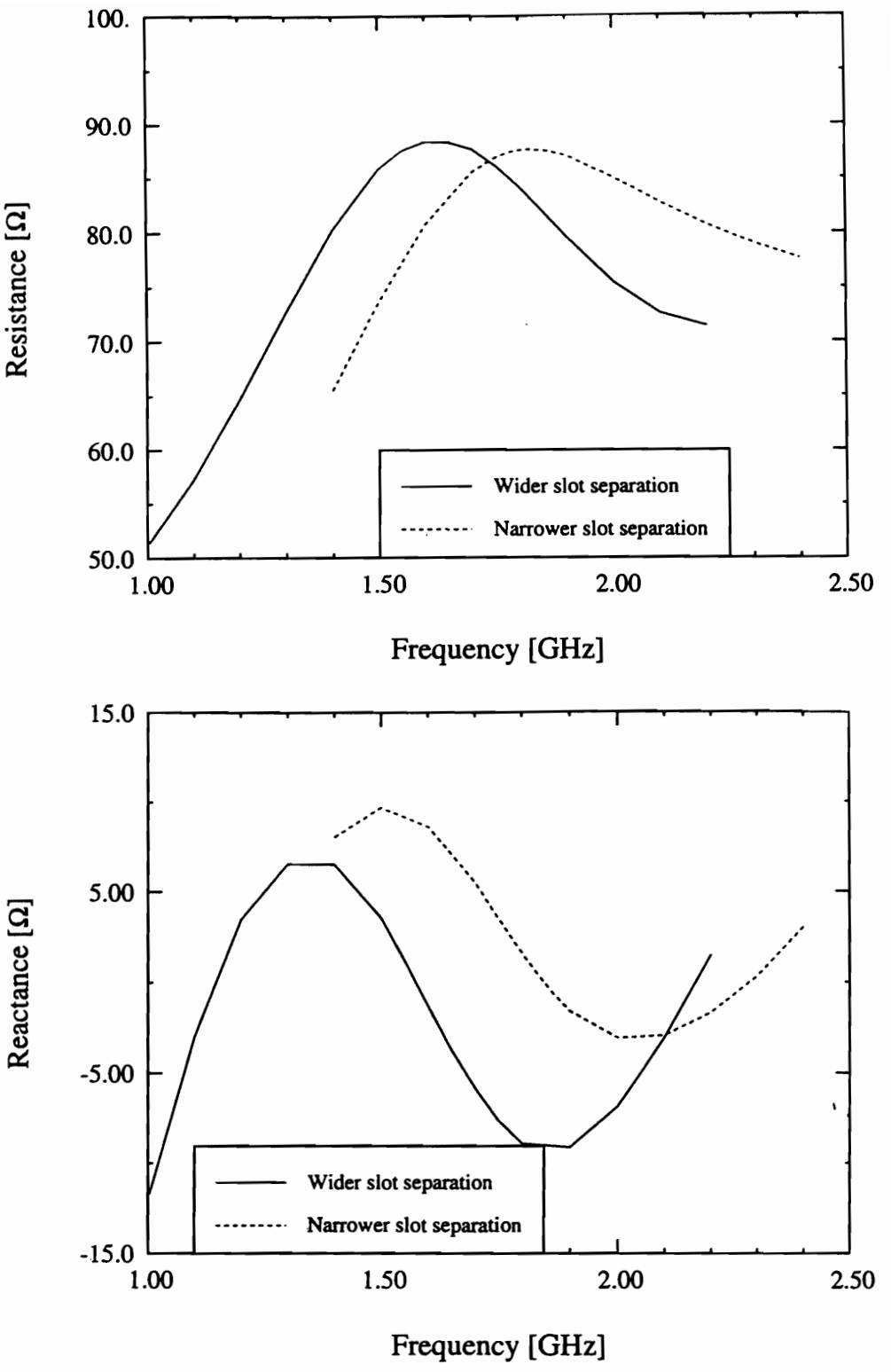

Figure 9: Variation of the input impedance of the folded slot with slot separation

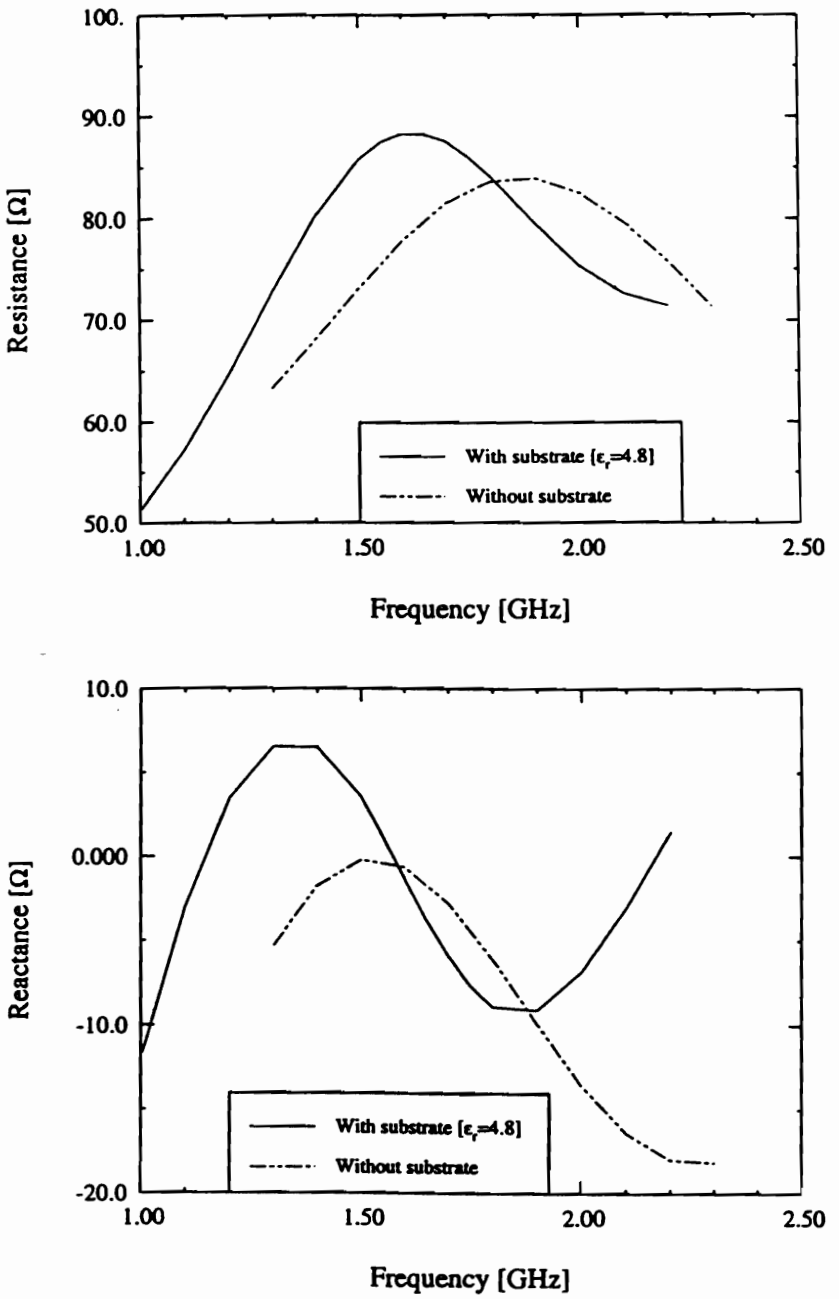

Figure 10: Effect of the presence of a substrate on the input impedance and resonant frequency of the folded slot

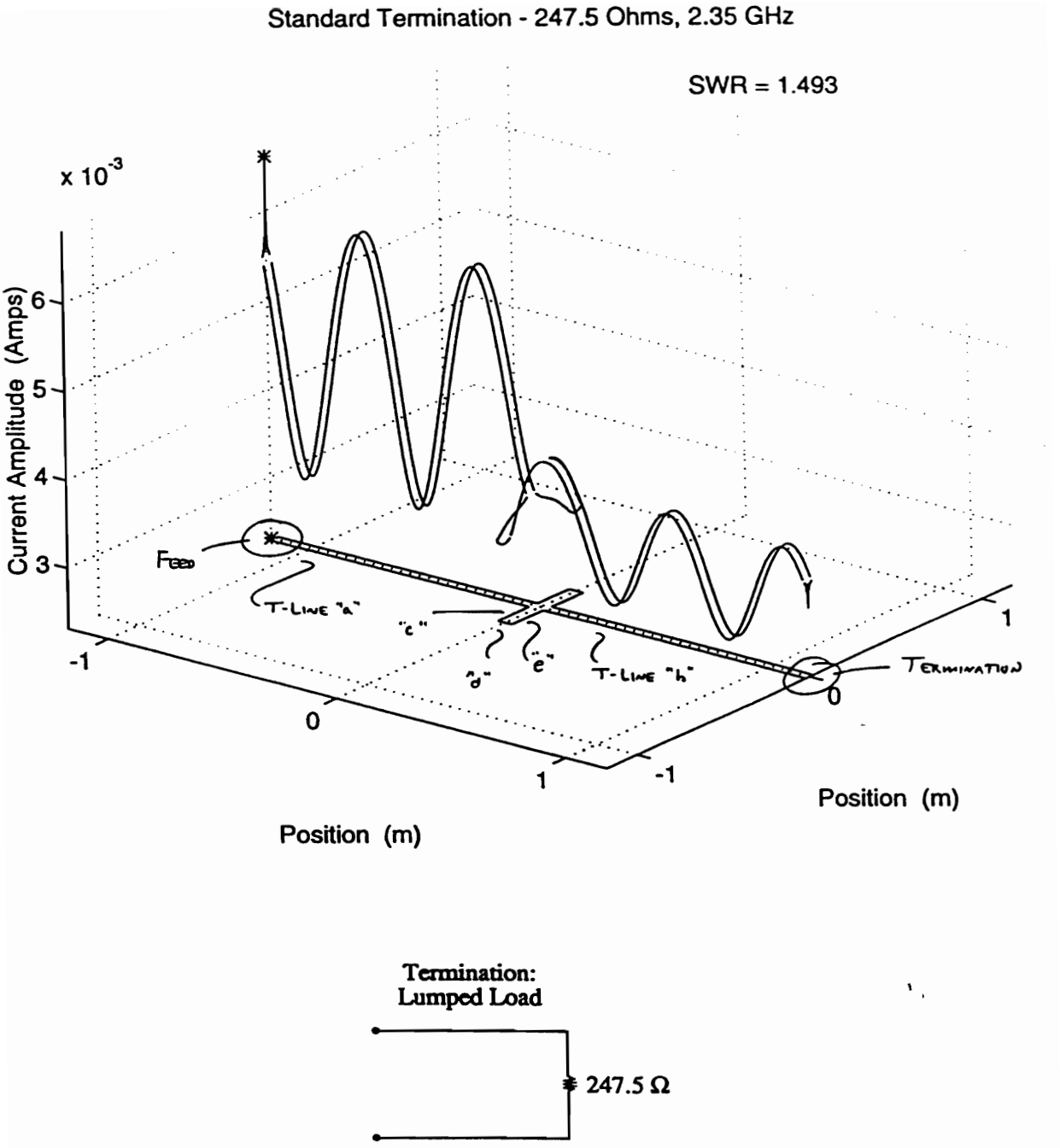

Figure 13: Initial test geometry and data, showing poor termination

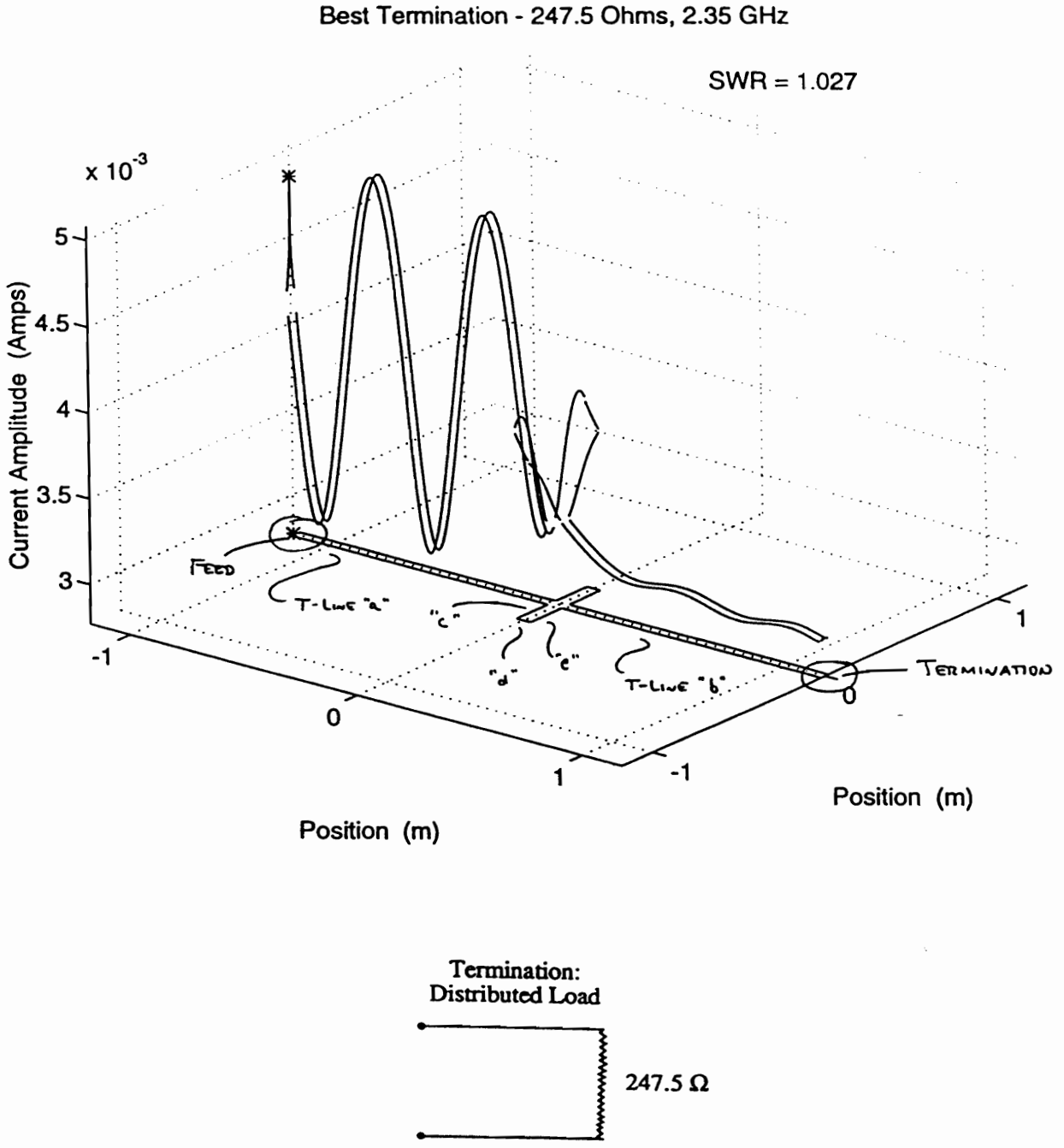

Figure 14: Final test geometry and data, showing optimized termination

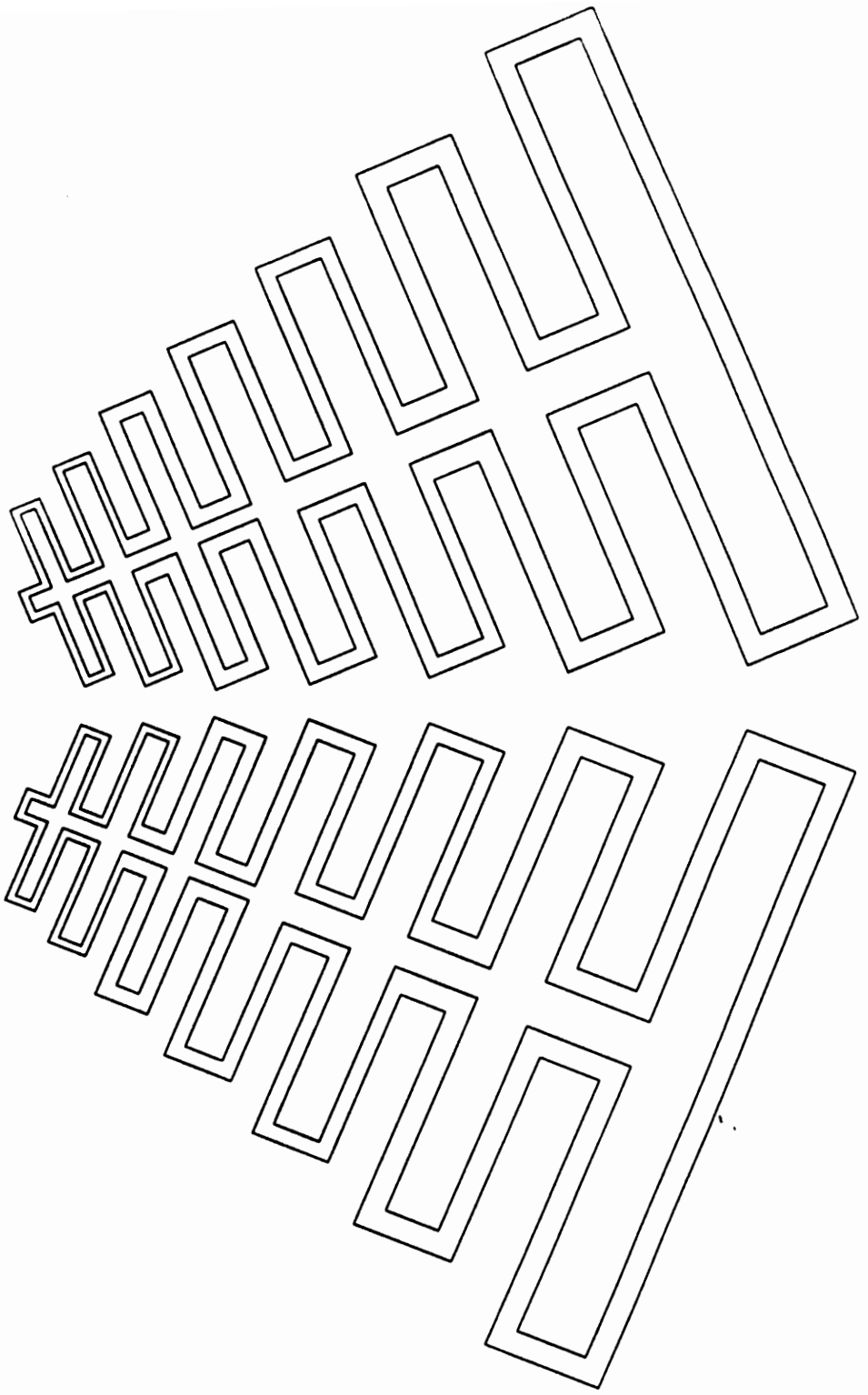

Figure 15: Geometry for coupling analysis

Array Directivity vs. Length

	Length		Gain
	cm	in.	(dB)
Present Design	8.4	3.3	8.2
20% longer	10.0	3.93	8.4
40% longer	11.7	4.61	8.6
75% longer	14.7	5.79	8.9
100% longer	16.8	6.61	9.2
150% longer	21.0	8.27	9.5
200% longer	25.2	9.92	9.8

Figure 16: Dependence of LPDA gain on array length

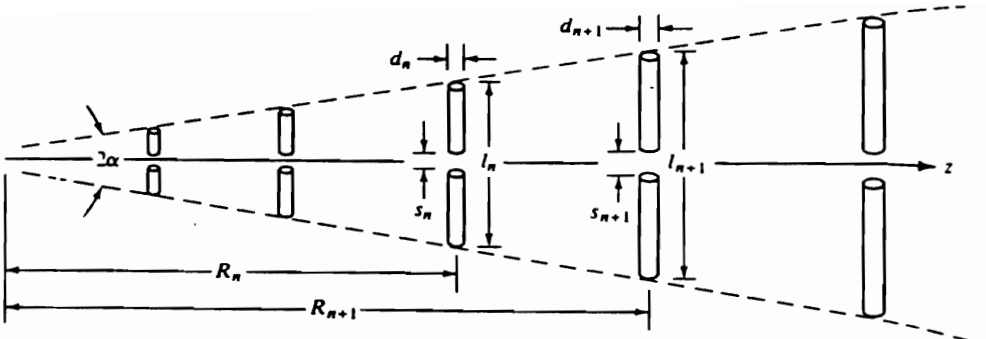

$$\tau = \frac{l_n}{l_{n+1}} = \frac{R_n}{R_{n+1}} = \frac{d_n}{d_{n+1}} = \frac{s_n}{s_{n+1}}$$

$$\sigma = \frac{R_{n+1} - R_n}{2l_{n+1}}$$

$$\alpha = \tan^{-1}\left[\frac{1-\tau}{4\sigma}\right]$$

Figure 17: LPDA design parameters and relations

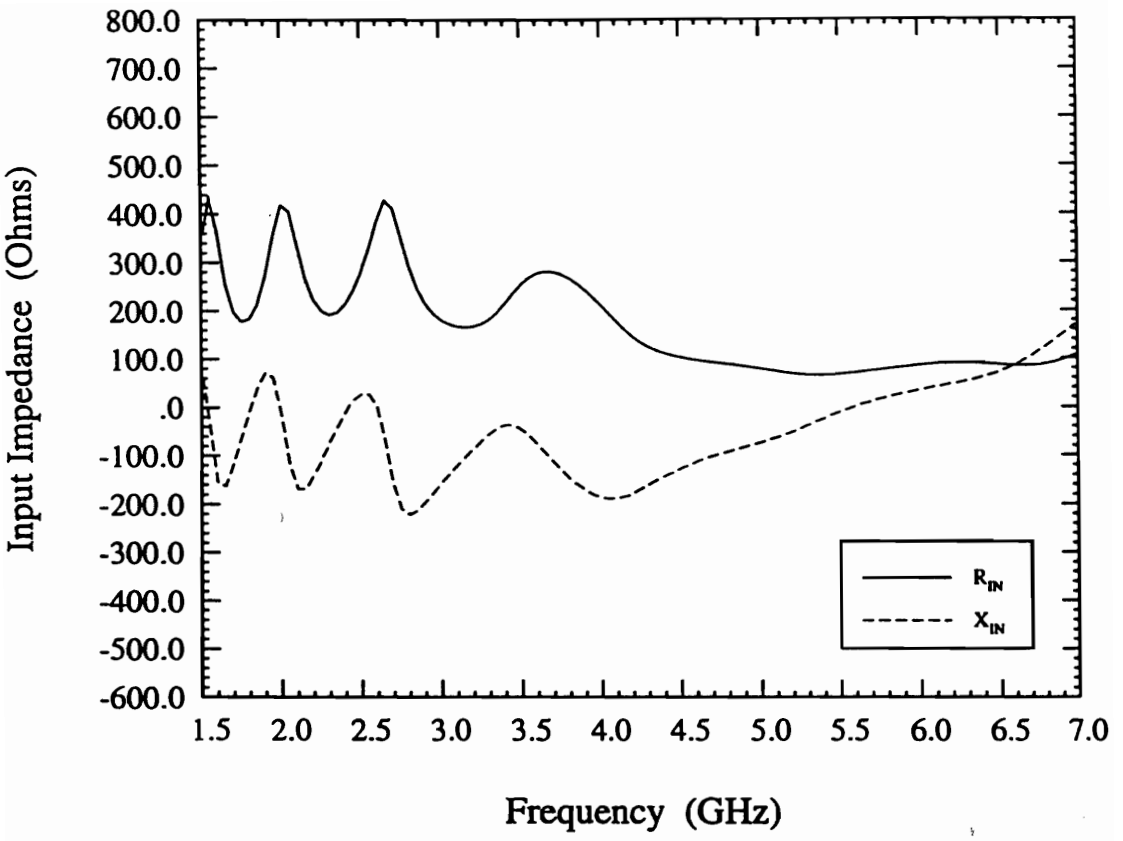

Figure 18: Input impedance for the equivalent theoretical LPDA

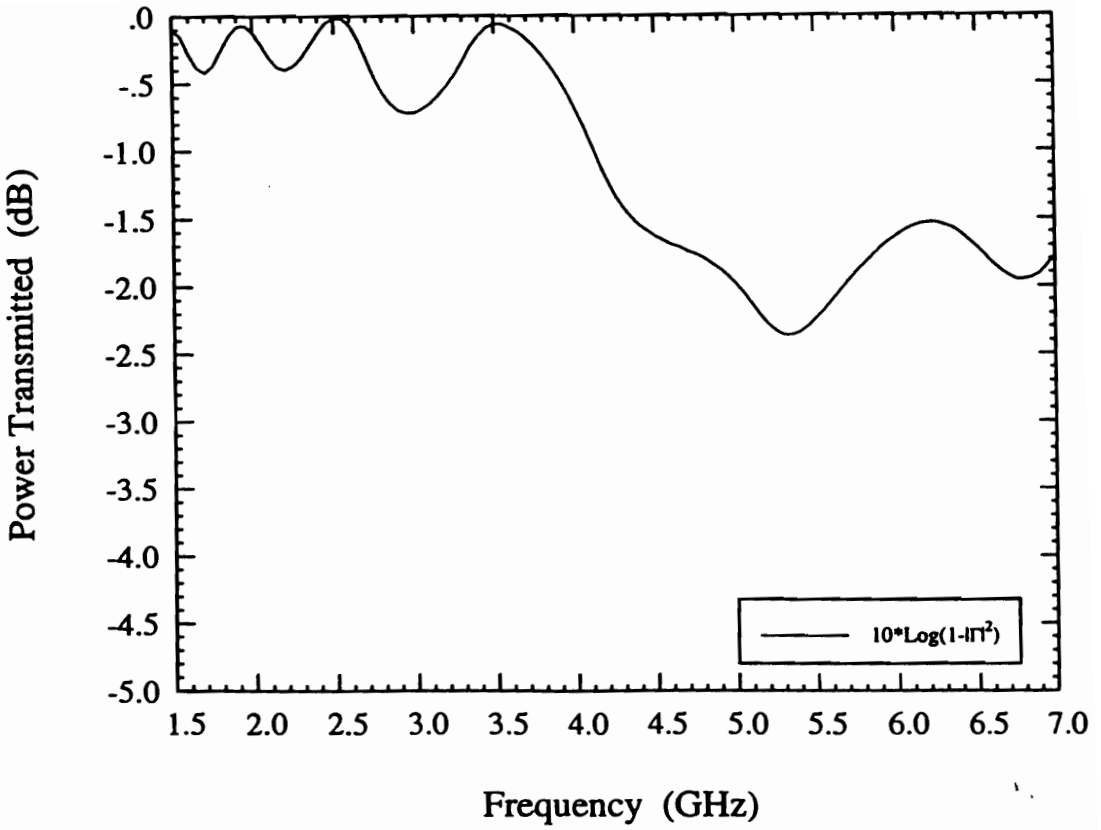

Figure 19: Transmitted power for the equivalent theoretical LPDA (see text)

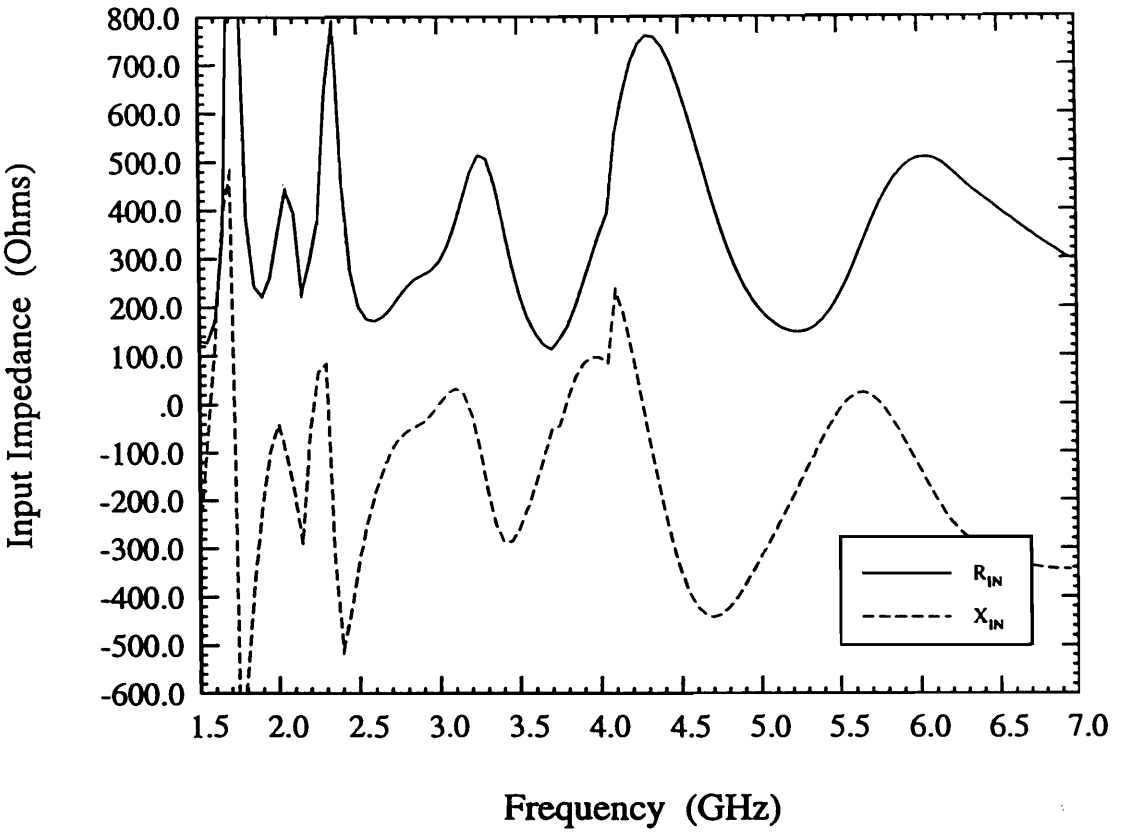

Figure 20: Input impedance for the LPFDA equivalent of the originally supplied LPFSA

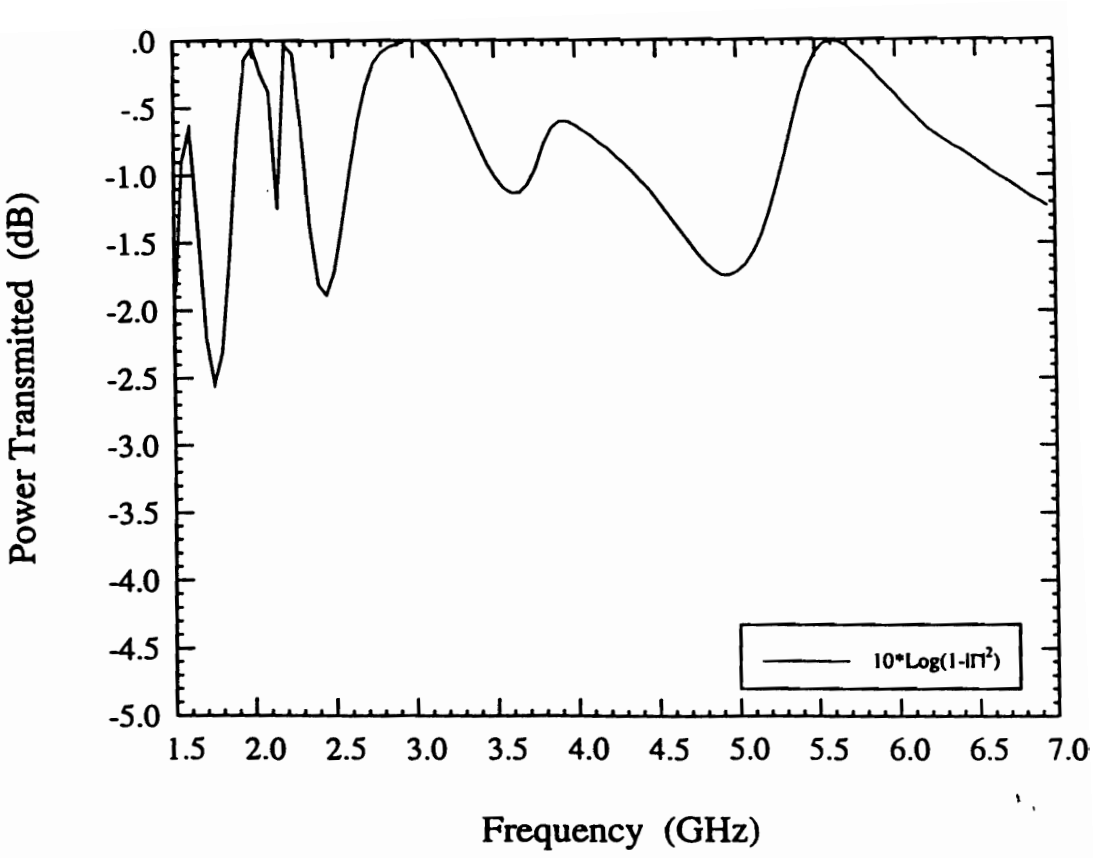

Figure 21: Transmitted power for the LPFDA equivalent of the originally supplied LPFSA

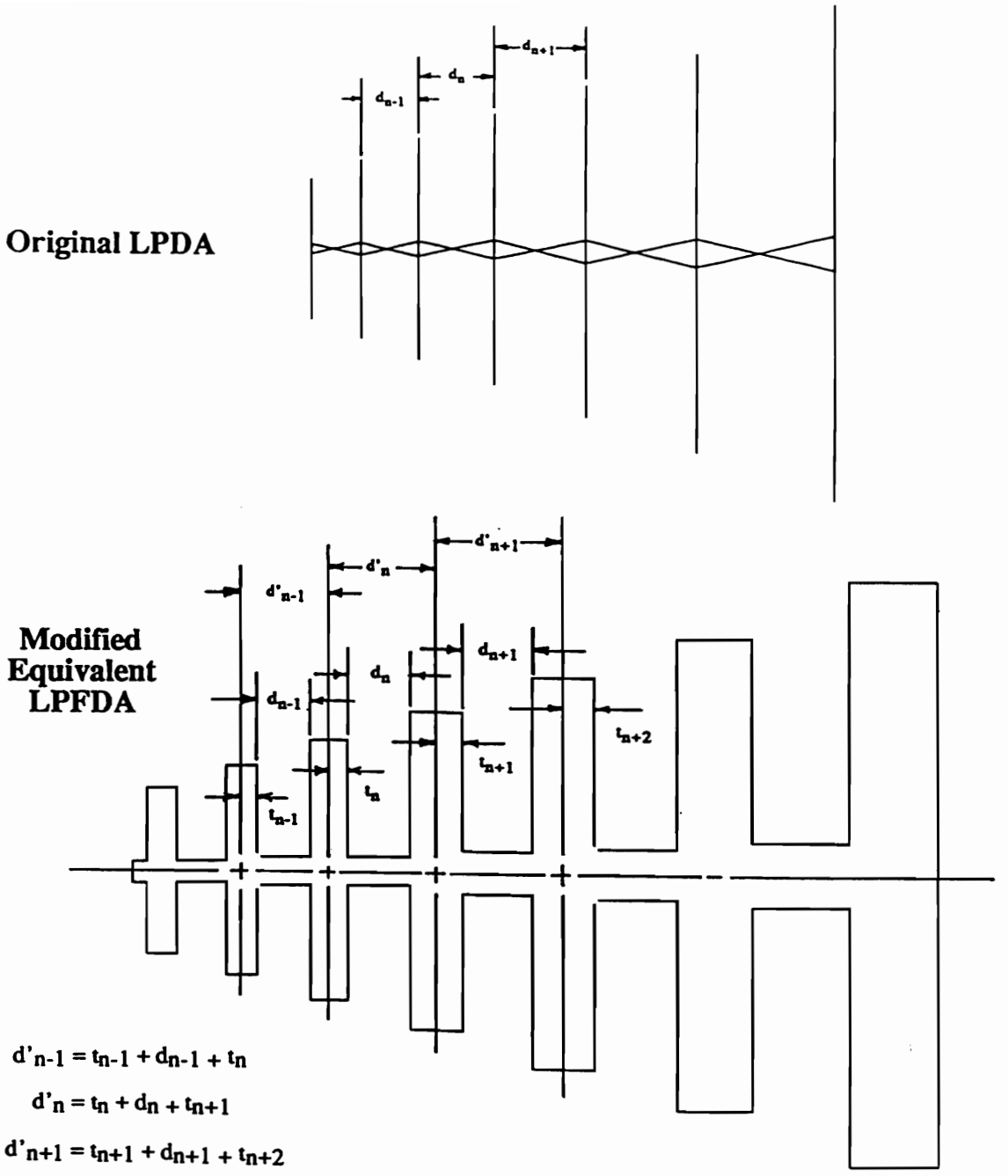

These modifications to the design procedure are currently being optimized.

Figure 22: Modified LPFDA design procedure and nomenclature

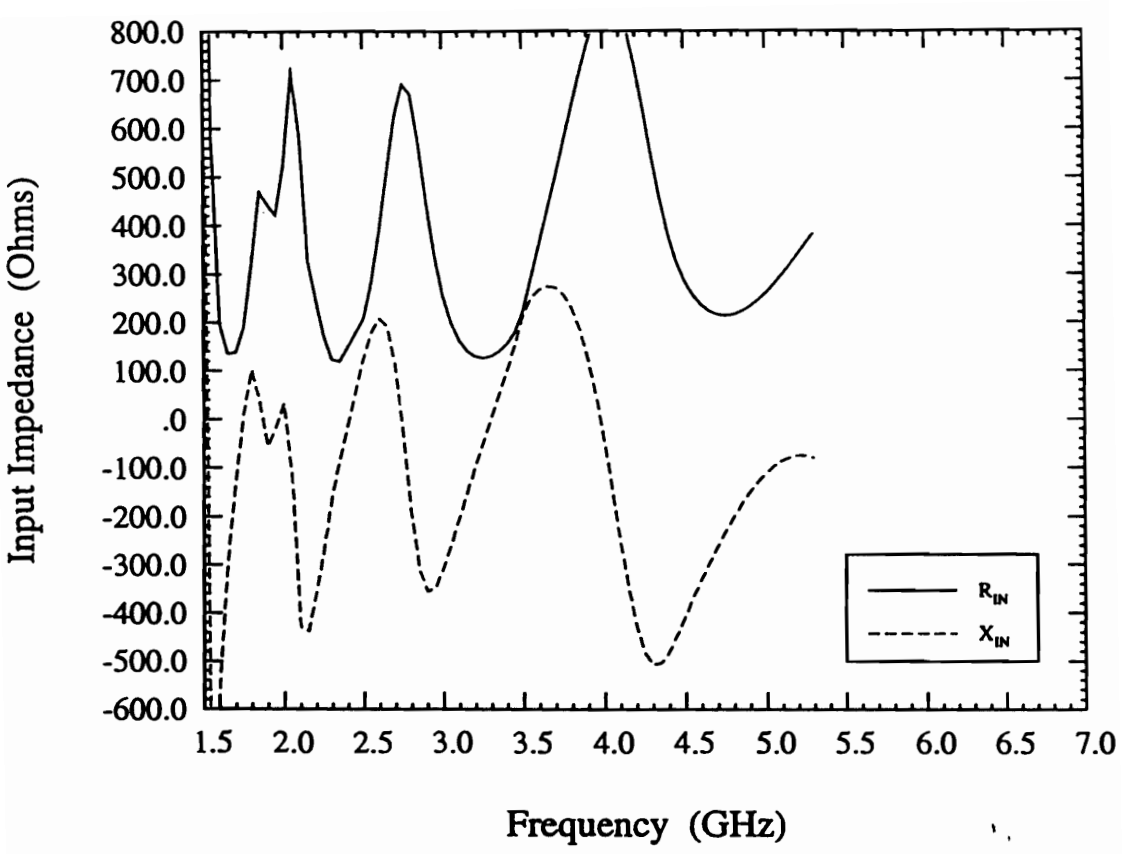

Figure 23: Input impedance for the modified LPFDA array

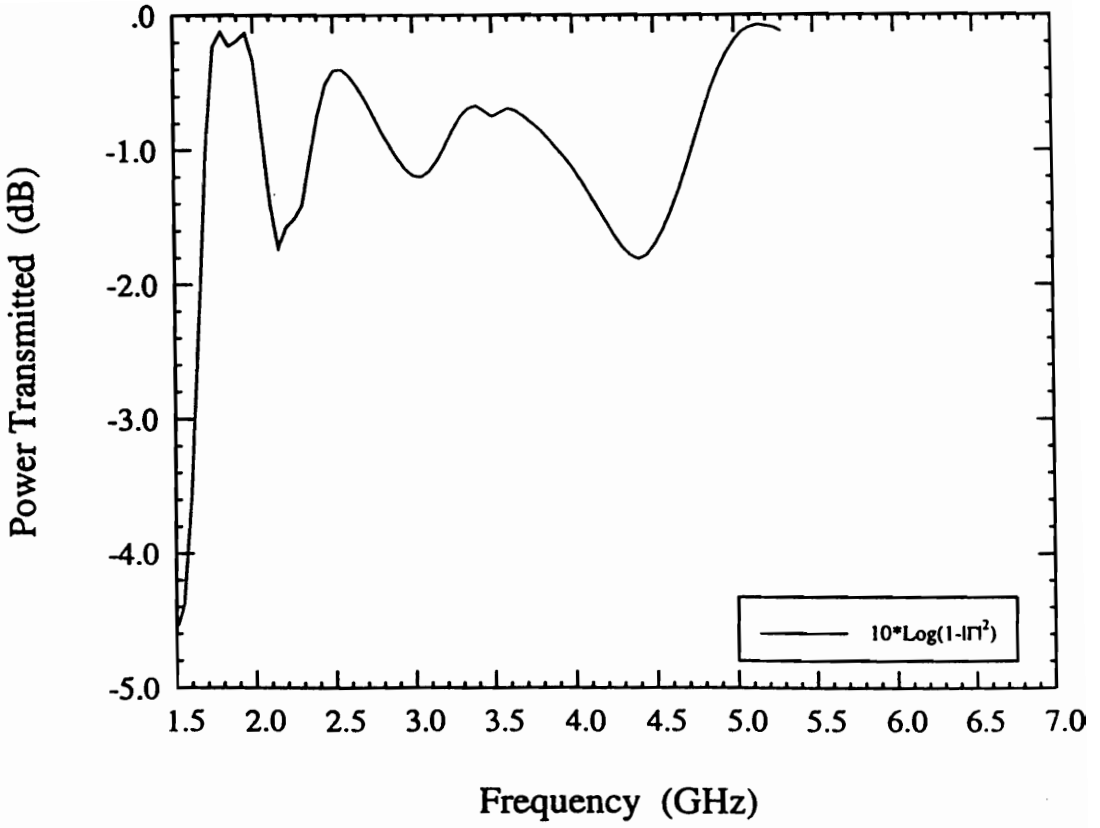

Figure 24: Transmitted power for the modified LPFDA array

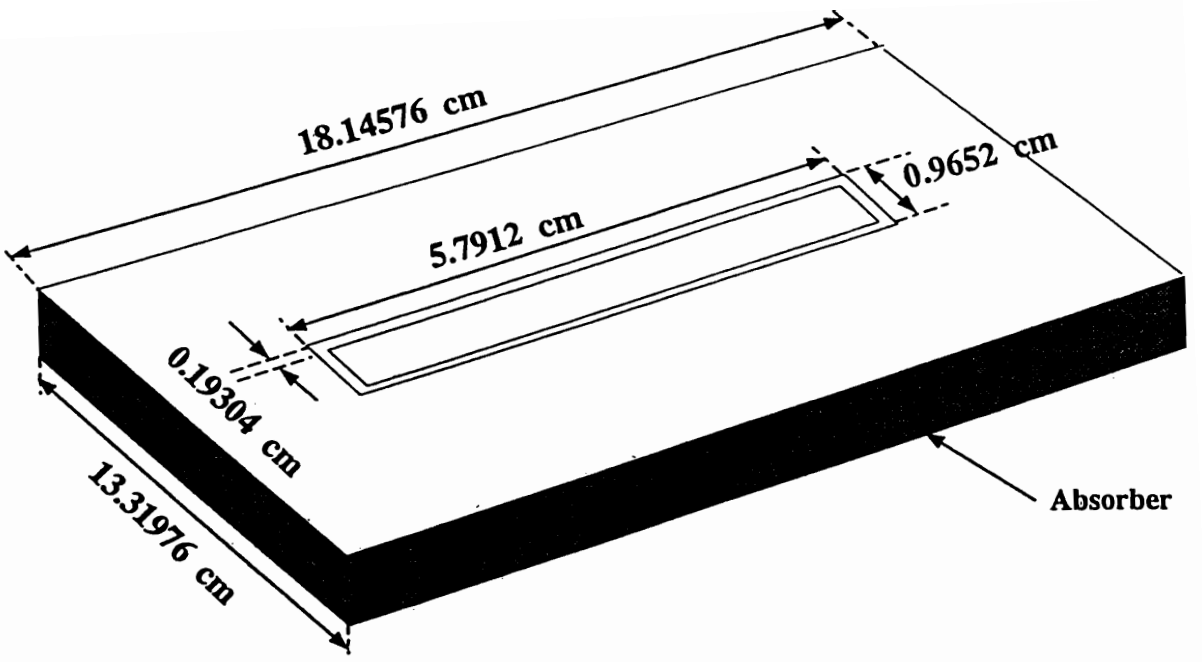

Figure 25: Geometry of the planar folded slot, showing the dielectric substrate

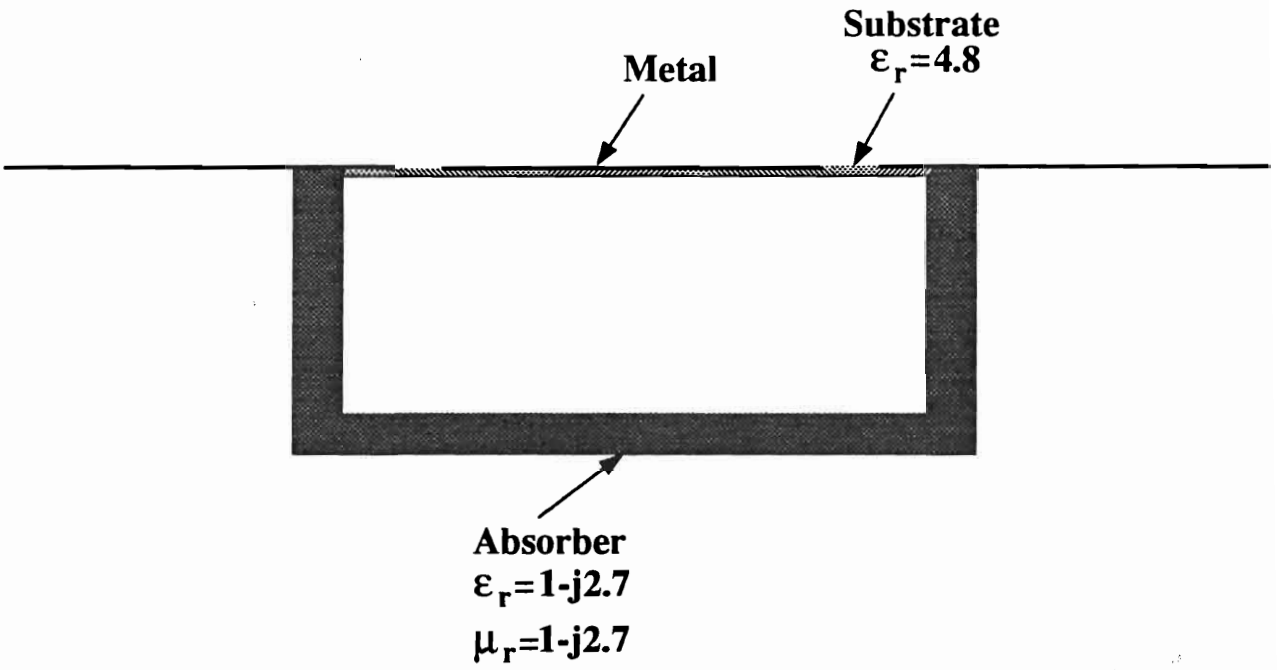

Figure 26: Geometry of the planar folded slot, showing the absorber-lined cavity

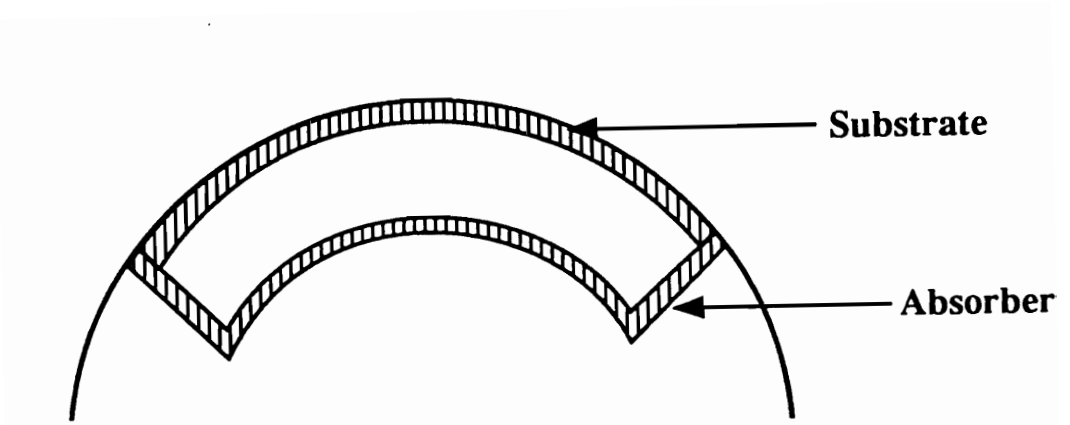

Figure 27: Geometry of the folded slot when mounted on a cylinder

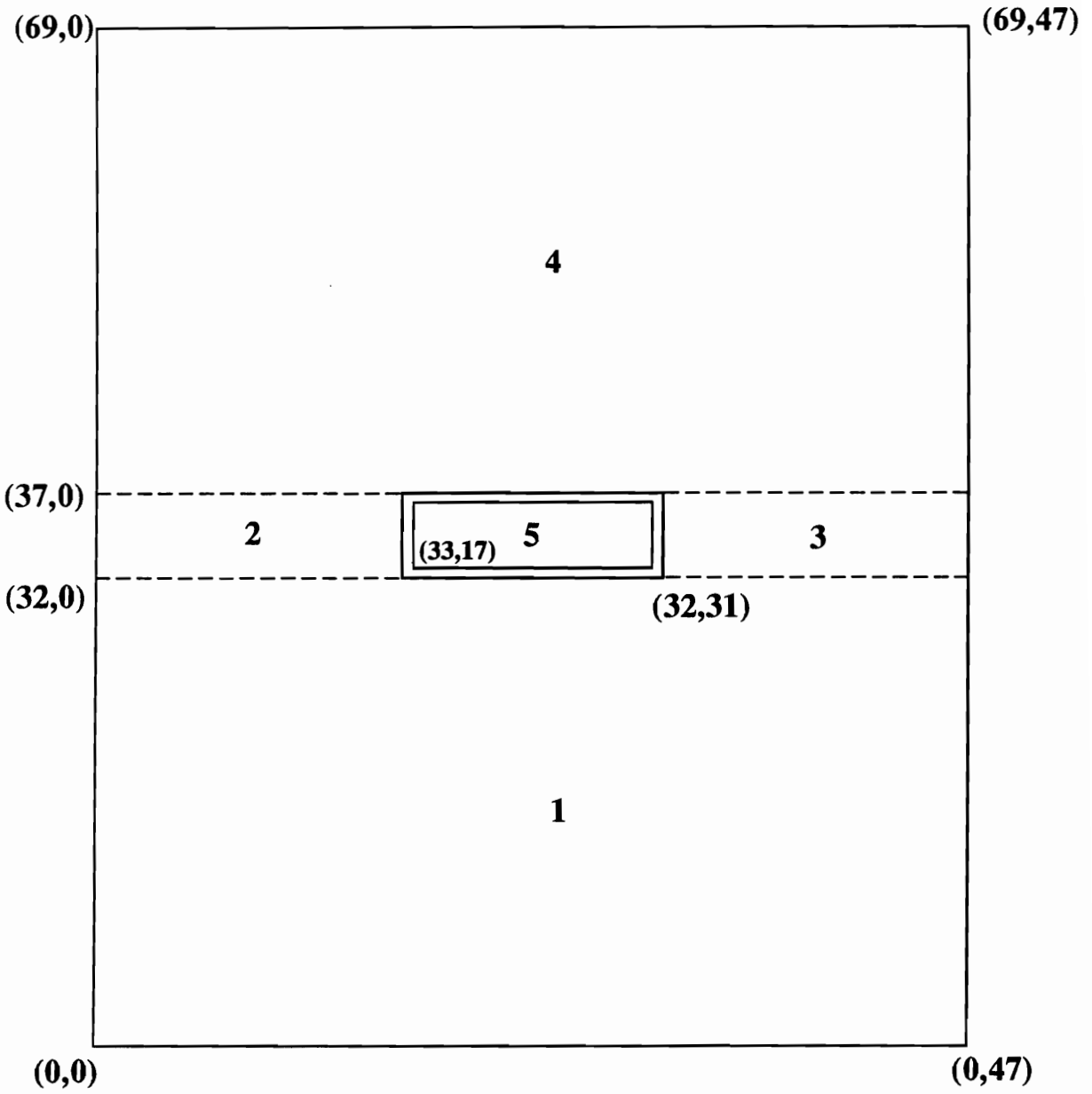

Figure 28: Modeling of the aperture as a collection of patches

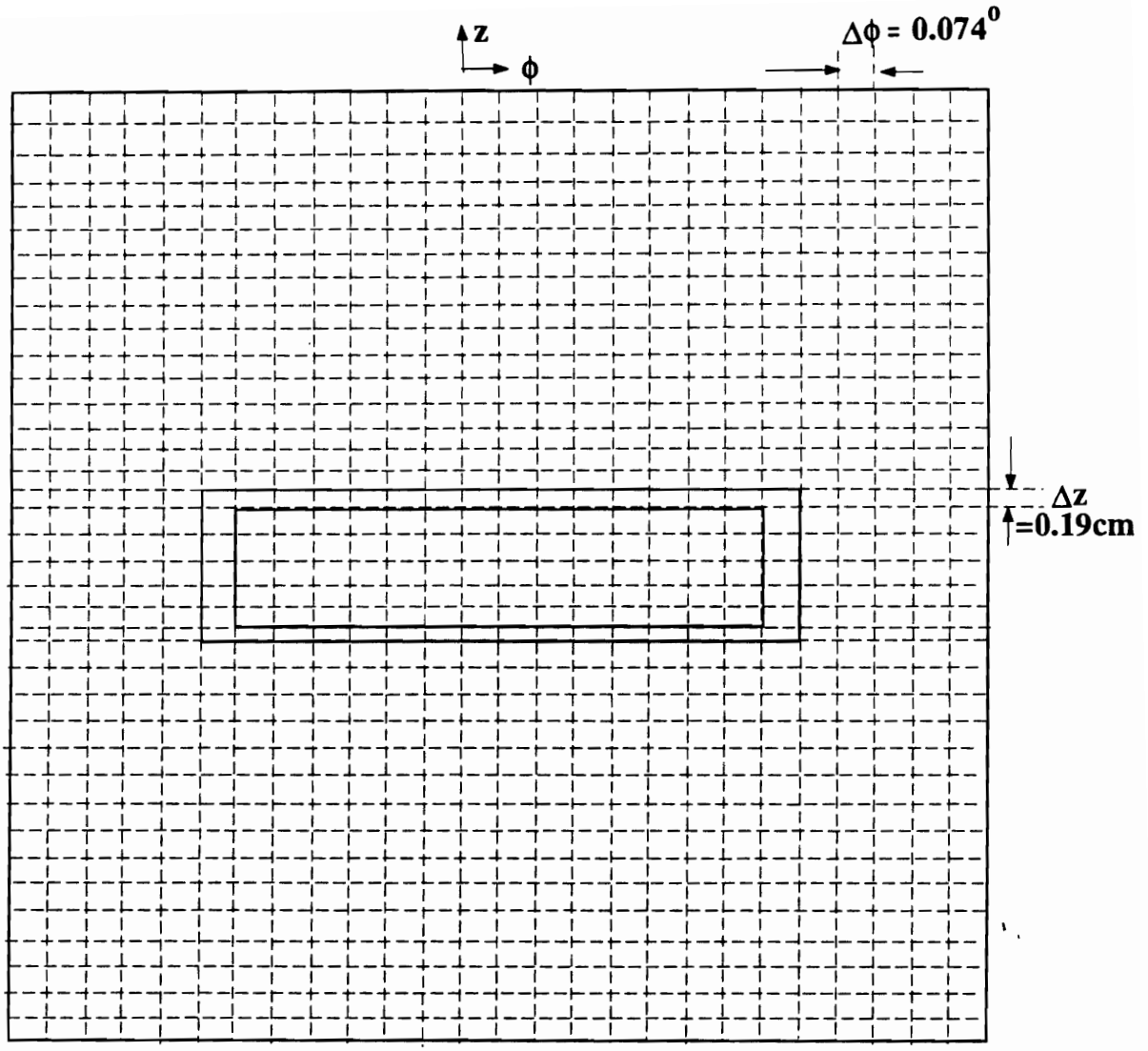

RUN STATISTICS :

NODES ~ 26,880
ELEMENTS ~ 22,701
METAL NODES ~ 3,428
EDGES ~ 76,336
INTERIOR EDGES ~ 60,116
METAL EDGES ~ 16,184
APERTURE EDGES ~ 36
UNKNOWNS ~ 60,152

Figure 29: Final discretization of the antenna aperture

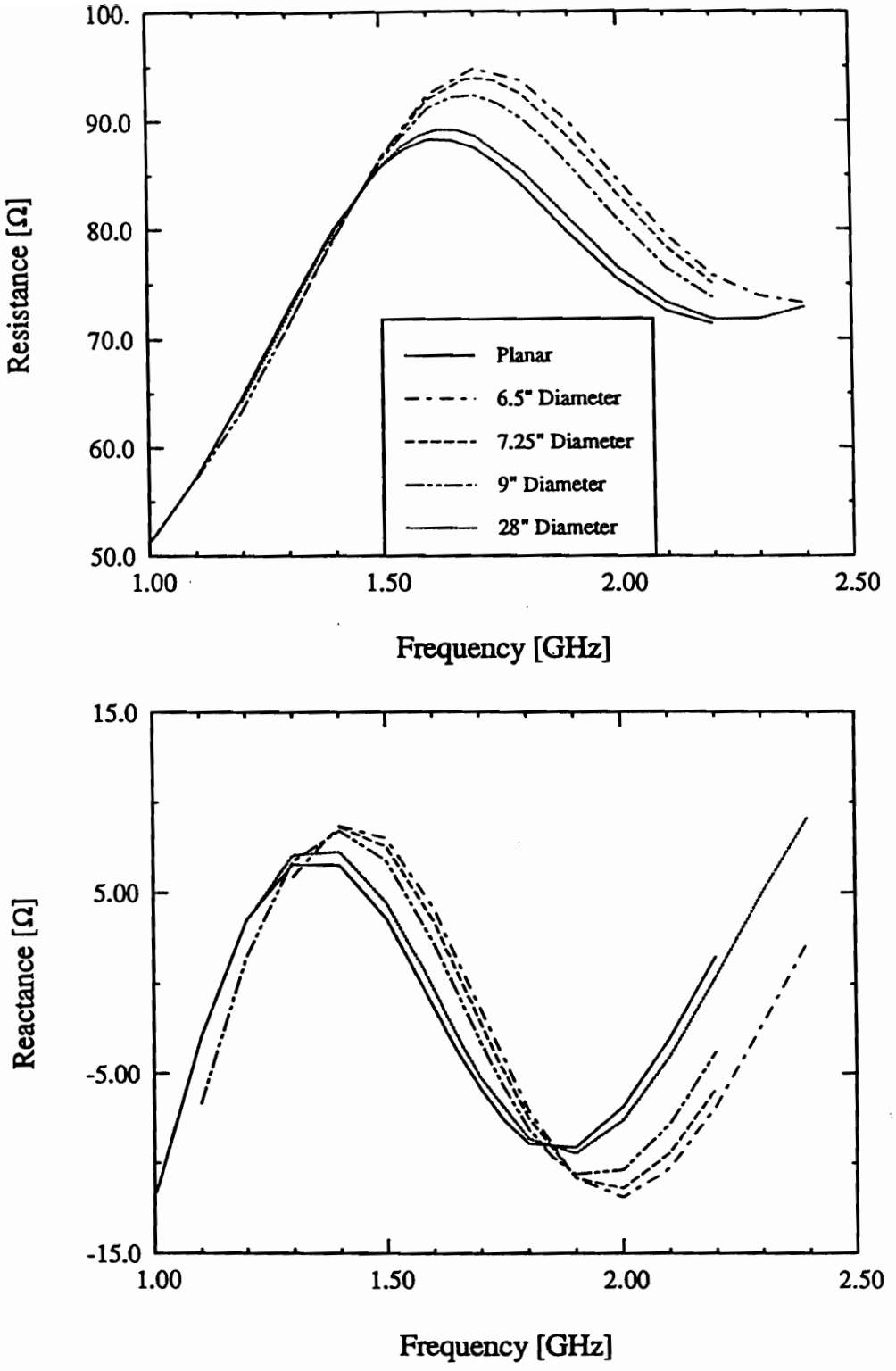

Figure 30: Input impedance of the large separation folded slot as a function of frequency

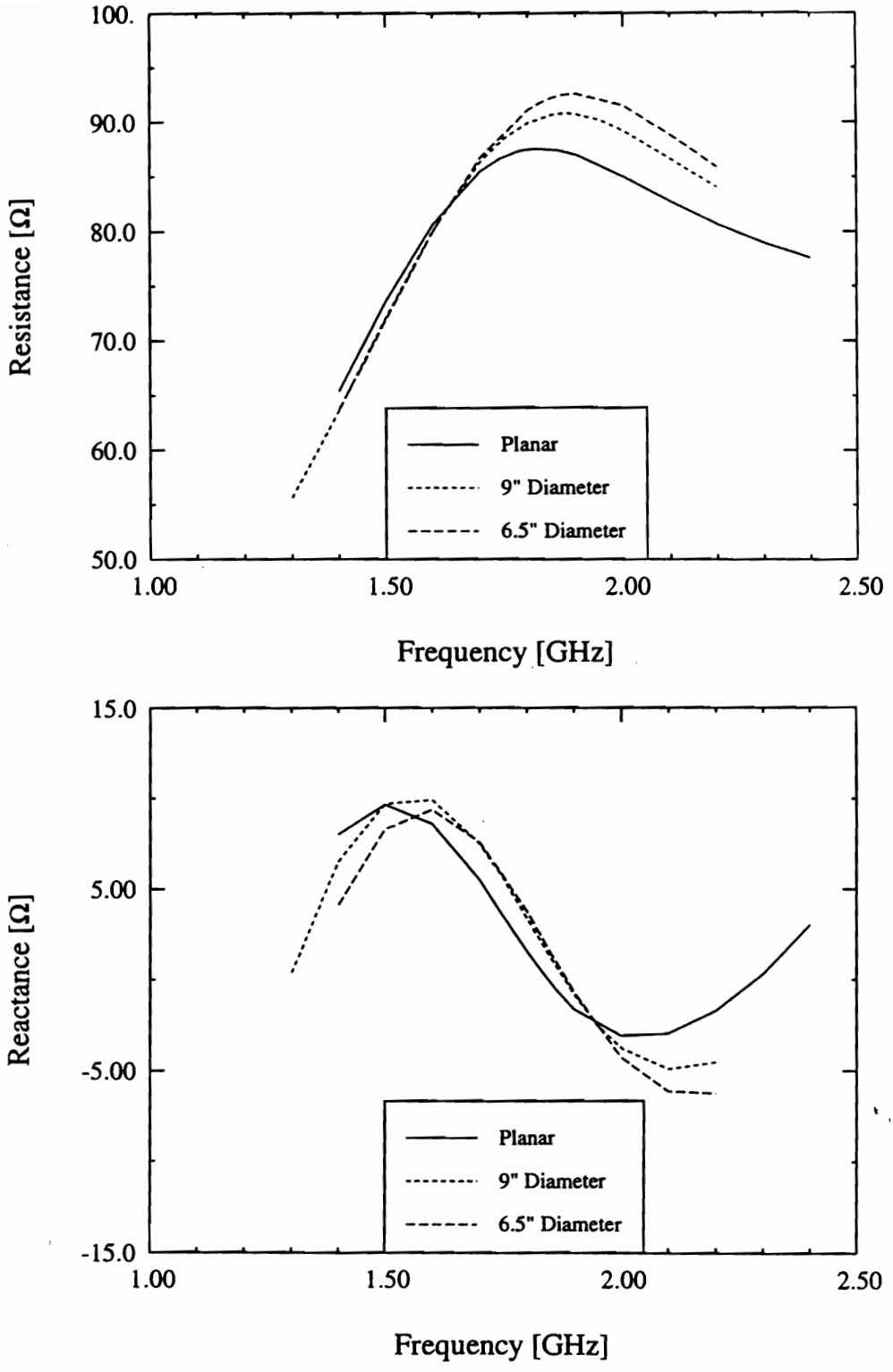

Figure 31: Input impedance of the narrow separation folded slot as a function of frequency

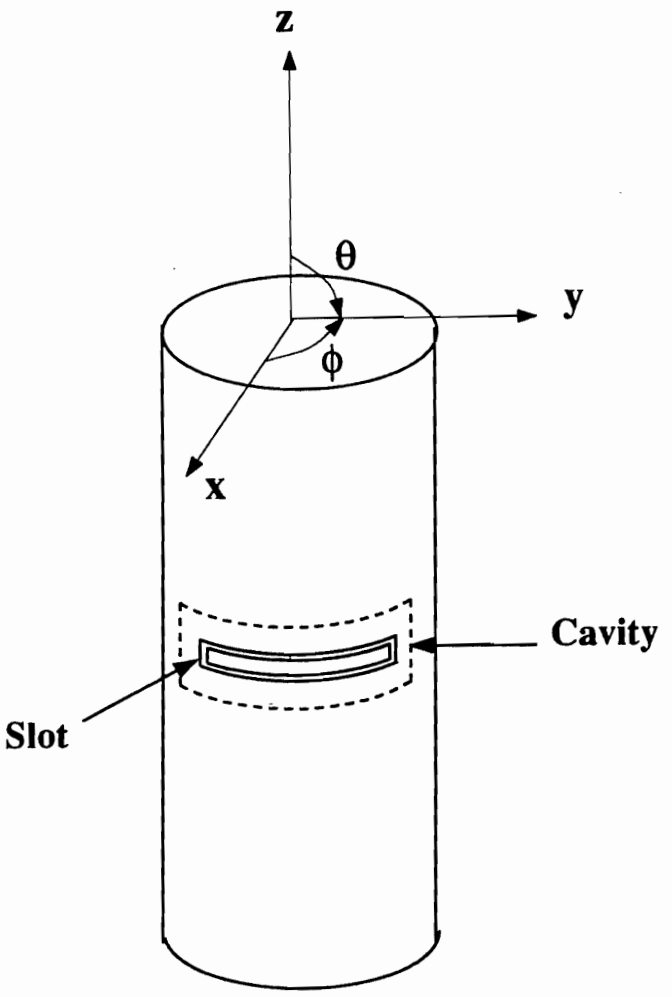

H-PLANE : $\theta = 90^0$; $\phi \longrightarrow$ -180^0 to 180^0

E-PLANE : $\phi = 0^0$; $\theta \longrightarrow$ 0^0 to 180^0

Figure 32: Principal plane definitions

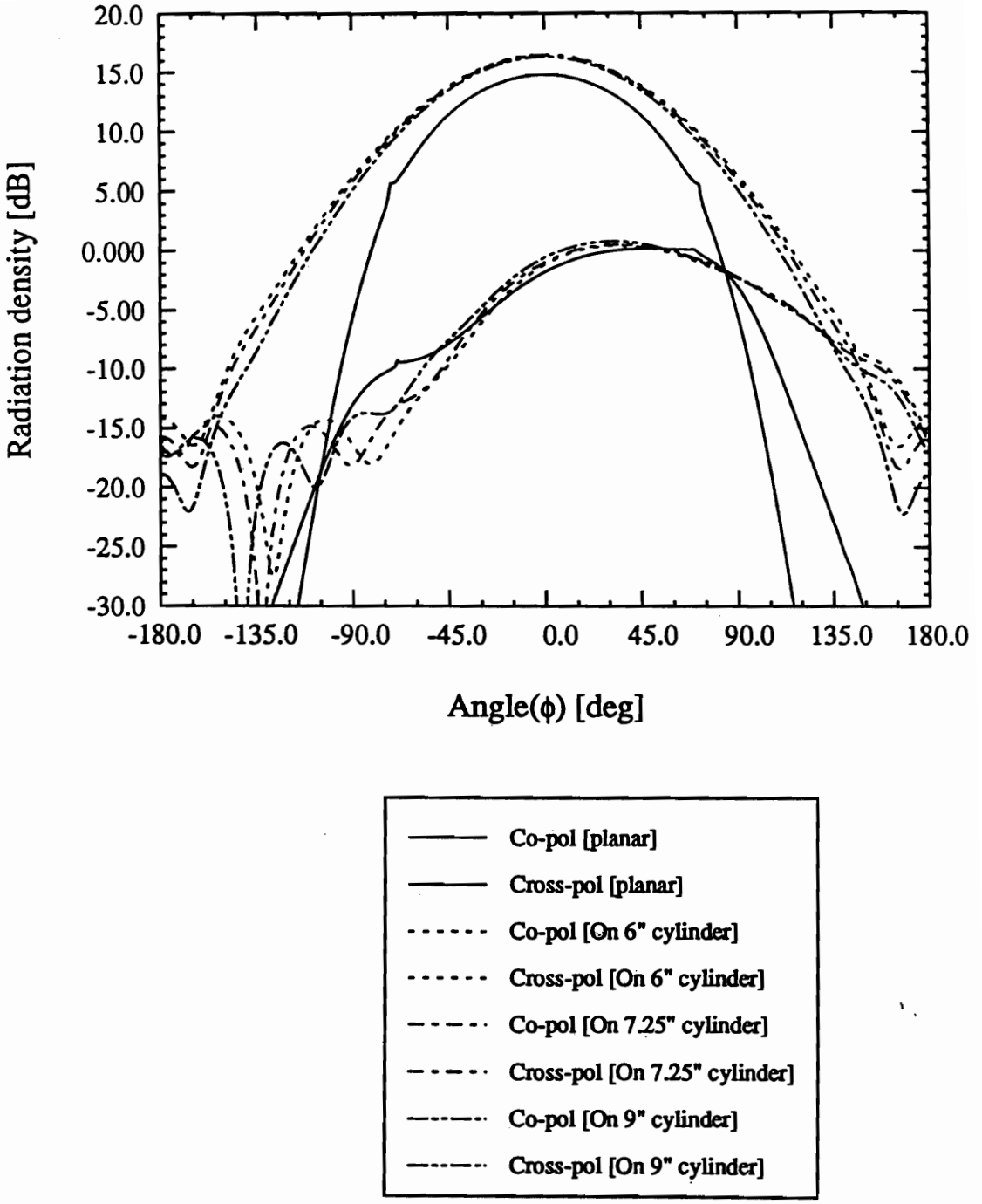

Figure 33: H-plane patterns for large separation slot as a function of curvature

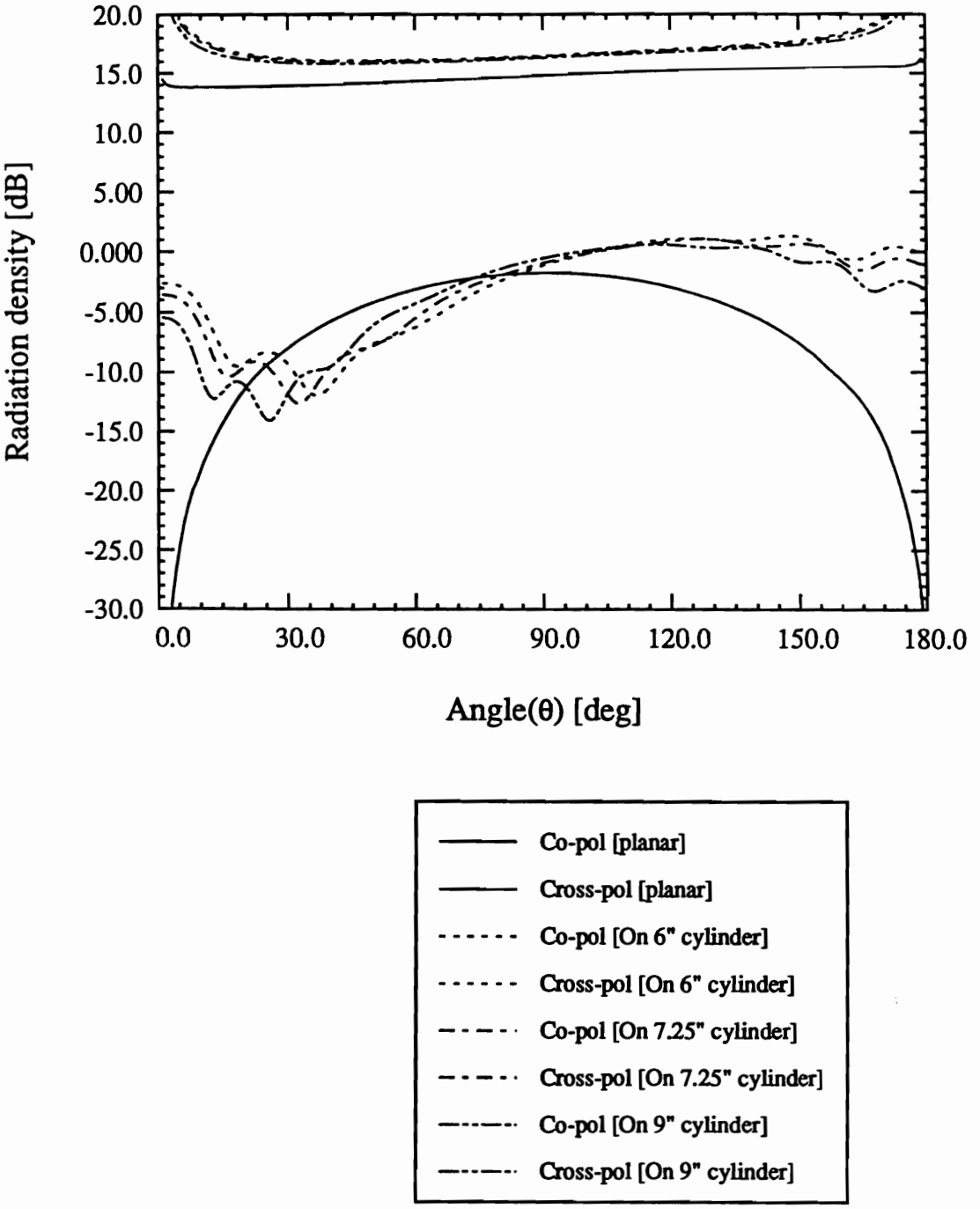

Figure 34: E-plane patterns for large separation slot as a function of curvature

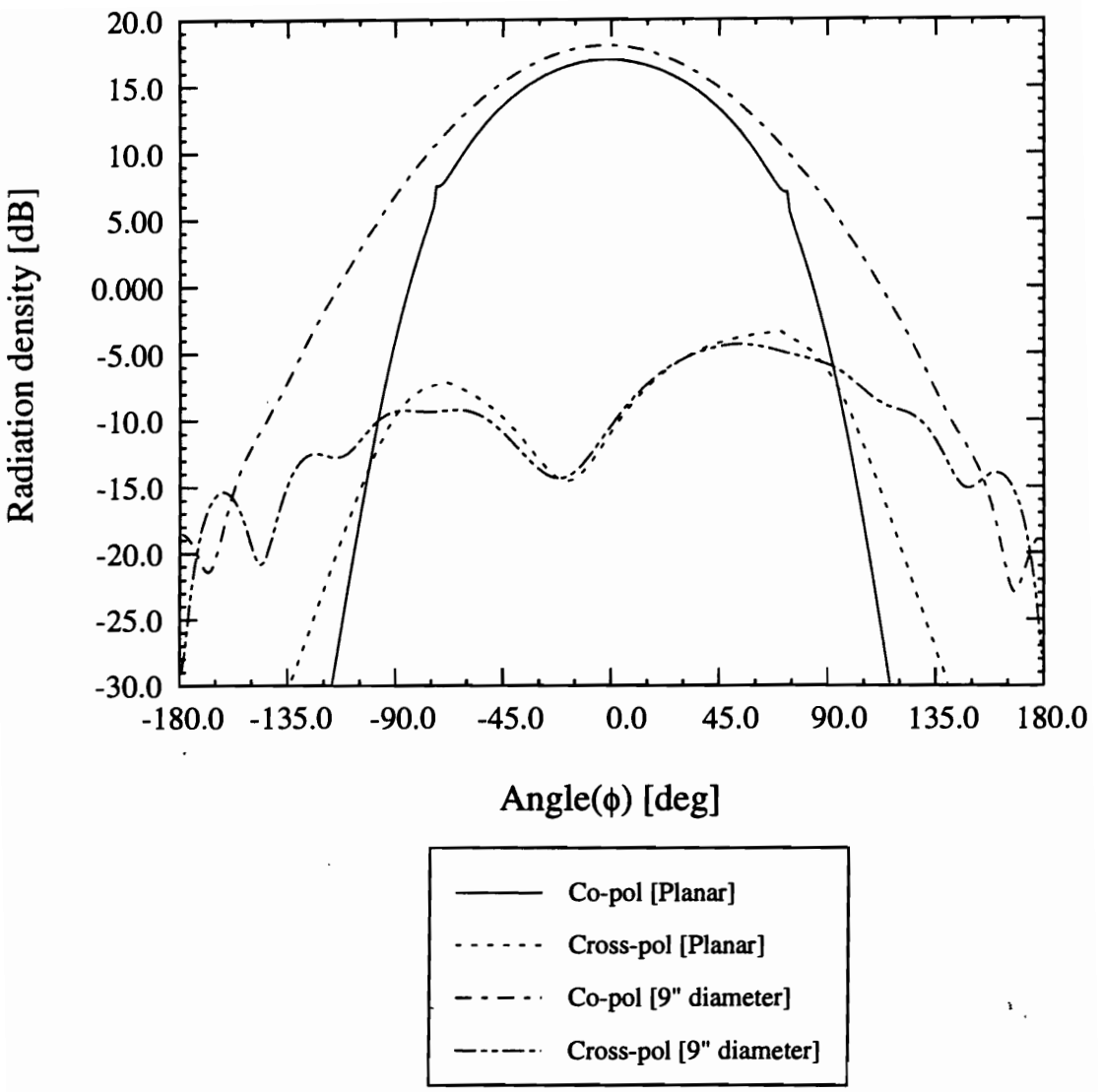

Figure 35: H-plane patterns for narrow separation slot as a function of curvature

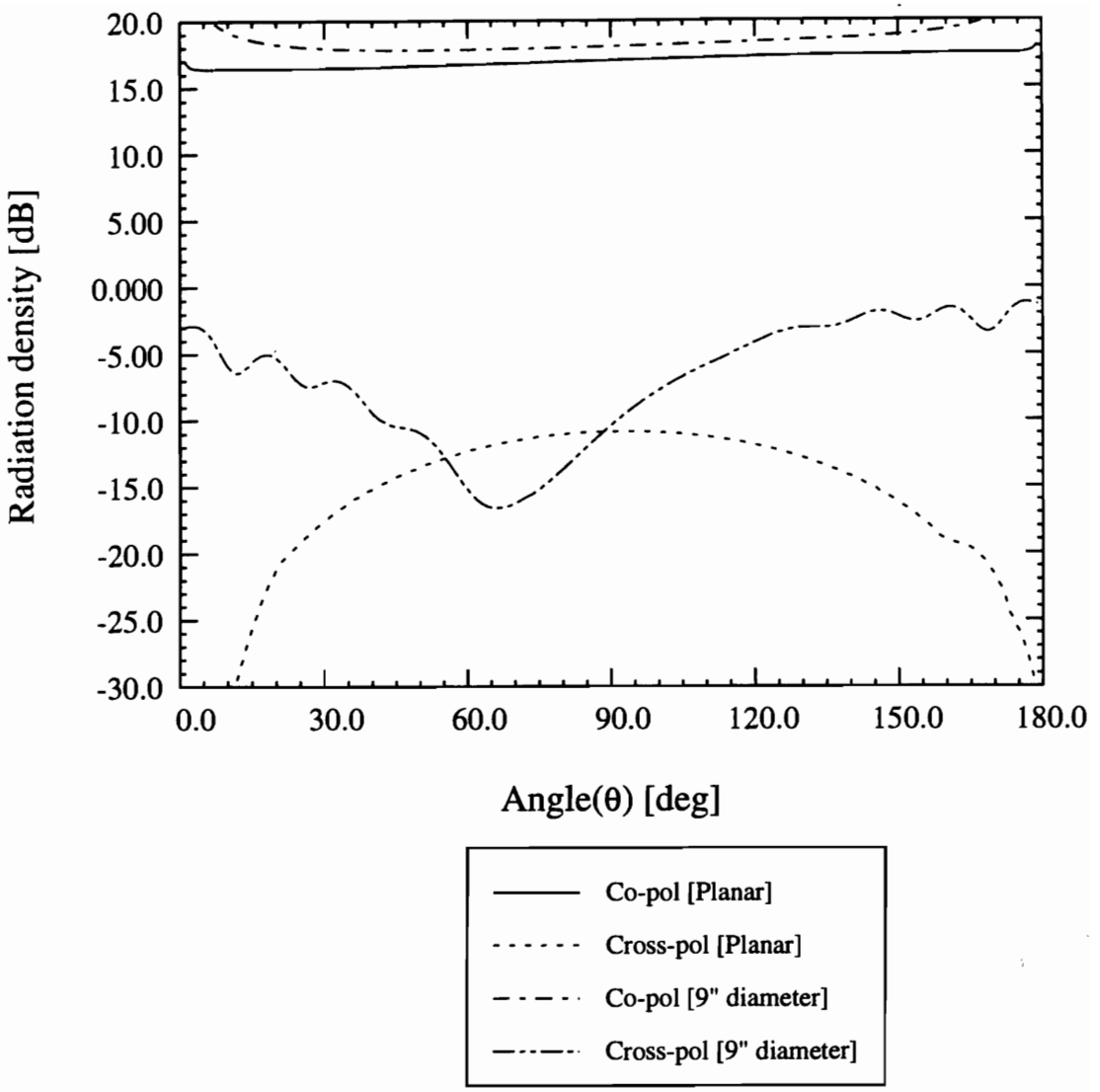

Figure 36: E-plane patterns for narrow separation slot as a function of curvature

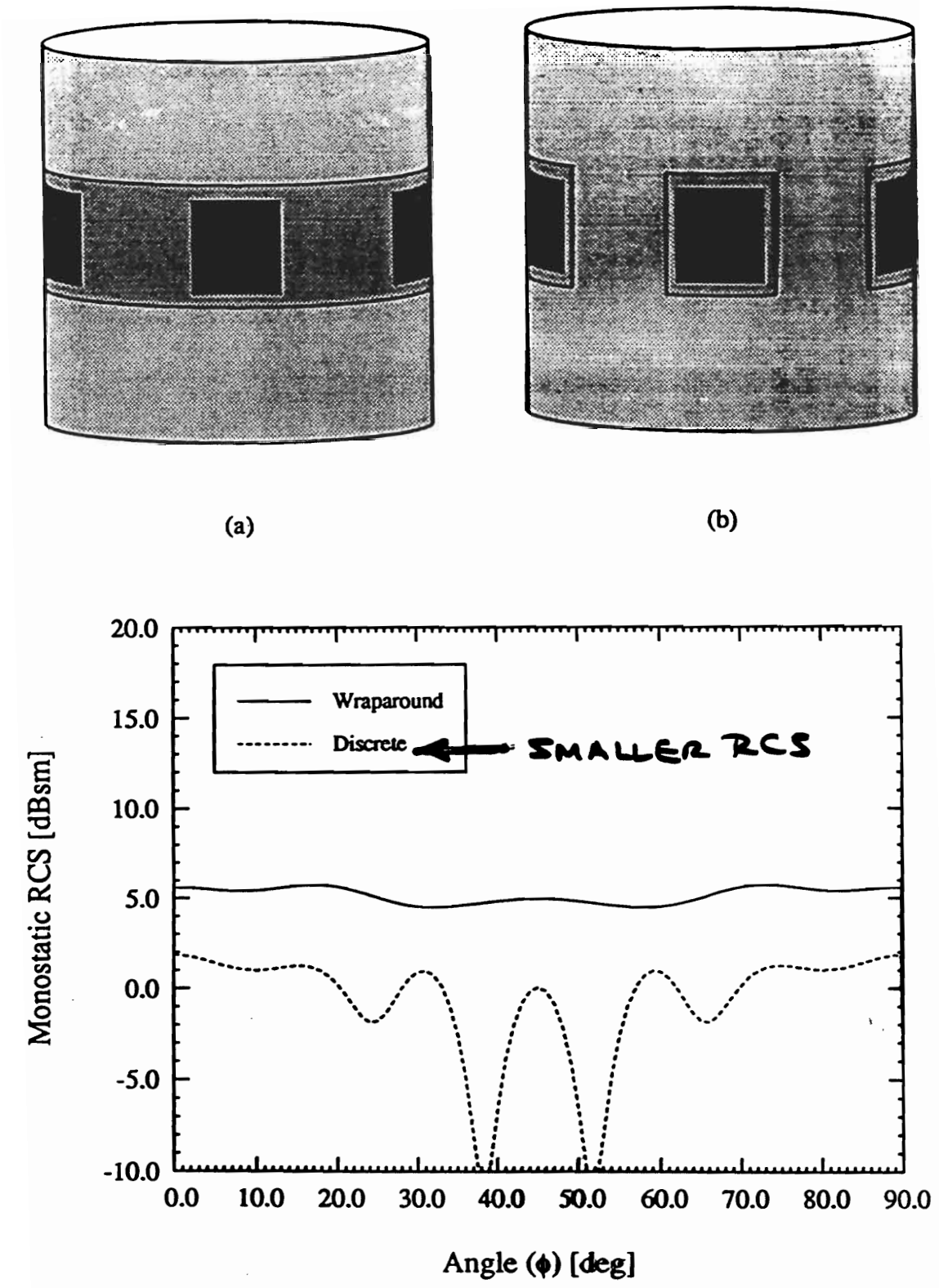

Figure 37: Necessity of separate backing cavities for each LPFSA